Contribution of Sentinel-2 satellite images for habitat mapping of the Natura 2000 site 'Estuaire de la Loire' (France)

M. Le Dez, Marc Robin, Patrick Launeau

Contribution of Sentinel-2 satellite images for habitat mapping of the Natura 2000 site 'Estuaire de la Loire' (France)

Mathieu Le Dez[a,c,*], Marc Robin[a], Patrick Launeau[b]

[a] *UMR CNRS 6554 LETG Littoral, Environnement, Télédétection, Géomatique – Université de Nantes, Chemin de la Censive du Tertre, B.P. 81227, 44312 Nantes, France*

[b] *UMR CNRS 6112 LPG Laboratoire de Planétologie et Géodynamique - Université de Nantes, 2 Rue de la Houssinière, B.P. 92208, 44322 Nantes, France*

[c] *Conseil Départemental de Loire-Atlantique – Unité milieux naturels Délégation Nantes – 26 Boulevard Victor Hugo, 44200 Nantes, France.*

***Corresponding author**

E-mail addresses : mathieu.ledez29@gmail.com (M. Le Dez), marc.robin@univ-nantes.fr (M. Robin), patrick.launeau@univ-nantes.fr (P. Launeau)

Keywords: Sentinel-2, Satellite multi-date classification, Natura 2000, Estuarine habitats, EUNIS habitat mapping, Phytosociology, Random Forest.

Abstract

Habitat mapping is an essential tool to implement the European Habitats Directive 92/43/EEC and to manage the Natura 2000 protected areas network. However, their elaboration is most often based on field surveys, which are time-consuming and expensive when dealing with large areas. In this study, we aimed to evaluate the contribution of Sentinel-2 satellite images for mapping habitats of the Natura 2000 site 'Estuaire de la Loire'. We used 1,248 phytosociological plots to establish a complete typology of the study site's habitats. Locating these plots led us to select training areas that characterize 39 habitats to calibrate the Random Forest algorithm. We classified 11 single-date images

spread evenly over a year and performed a multi-date classification of 9 images. We obtained high overall accuracy between 76.47% and 87.28% for the single-date image classifications and 98.7% for multi-date image classification. Our results demonstrate that Sentinel-2 images are appropriate for accurate habitat mapping and constitute a relevant tool to identify and conserve habitats of community interest.

1. Introduction

Preserving habitats is a major challenge for European nature conservation policies (Bijlsma et al., 2019). The implementation of the Habitats Directive 92/43/CEE (HabDir) especially permitted to target the most threatened habitats for which the European Union (EU) is committed to ensuring the maintain or the restoration to a favorable state of conservation (Art. 2 of HabDir) (Evans & Arvela 2011; Schaminée et al., 2016). Moreover, the Directive imposes applying measures of conservation and assessing the state of these habitats regularly. More specifically, naming protected areas led to the creation of the Natura 2000 network for which it is necessary to gather information on the habitats' distribution and surface areas (Evans, 2012).

To meet this goal, the EU member states need precise, simple and reproducible methods. Mapping represents an excellent tool to evaluate the habitat distribution and surface areas (Bunce et al., 2013). Currently, mapping methodologies are mainly based on field surveys and photo-interpretation (Ichter et al., 2014). These methods require roaming all the study areas to gather data on the vegetation and environmental factors characterizing the habitats. However, this type of mapping becomes quickly very time-consuming, costly and therefore difficult to implement in large and difficult-to-access territories (Kopeć et al., 2016; Moran et al., 2017). This is especially the case when mapping wetlands, which tend to be inaccessible because of numerous canals and flooded areas. (Harris et al., 2015; Zlinszky et al., 2014). Furthermore, this type of work is often subjective, which is why the cartographic productions can greatly vary from one operator to the other (Cherrill, 2014; Raab et al., 2018; Ullerud et al., 2018).

Approaches based on remote sensing currently offer many opportunities for cost-effective, rapid and reproducible mapping (Corbane et al., 2015; Vanden Borre et al., 2011). More and more studies show that remote sensing is increasingly used for mapping natural environments (Lang et al., 2015). For example, this is the case for studies on the mapping of alkaline peatland habitats in Poland using Rapid-Eye satellite images (Stenzel et al., 2014) or on mapping Belgian heathland habitats using hyperspectral airborne imagery (Haest et al., 2017). The quality of the remote sensing-based image classification depends on the characteristics of the images used, like the number of available spectral bands, the spatial resolution or the sensor's acquisition frequency. The Sentinel-2 satellite constellation produces 13-band multispectral images in the visible and infrared frequency range with a minimum spatial resolution of 100 m² and a high revisit frequency (several images per month). These characteristics are a good compromise for mapping wetland vegetation, in particular through multi-date classifications (Rapinel et al., 2019; Vrieling et al., 2018). To overcome these obstacles, remote sensing is a pertinent tool for identifying and locating habitats and, more broadly, areas with conservation issues. In this context, this study aims to assess the contribution of Sentinel-2 satellite images to mapping habitats in the Loire estuary by (1) developing an exhaustive typology of habitats from ground reference data and by (2) testing the accuracy of single-date and multi-date Sentinel-2 image classification using the Random Forest algorithm.

2. Materials and Methods

2.1 Study area

The Natura 2000 site 'Estuaire de la Loire', located in western France (47° 15′N, 1° 54′O) (Fig. 1), is an estuary formed by the Loire's alluvial plain which covers an area of 26,000 ha. It is a tidal wetland site of major ecological importance, hence its designation in 2004 as a Natura 2000 site (FR5200621 – Estuaire de la Loire). The site is recognized for the diversity of its ecosystems, from coastal habitats of dunes and salt marshes to agropastoral habitats of freshwater marshes and woodland habitats. The

large variety of habitats is mostly linked to flood frequency and duration, variations in exposure to salinity, as well as agricultural management (mainly mowing and grazing).

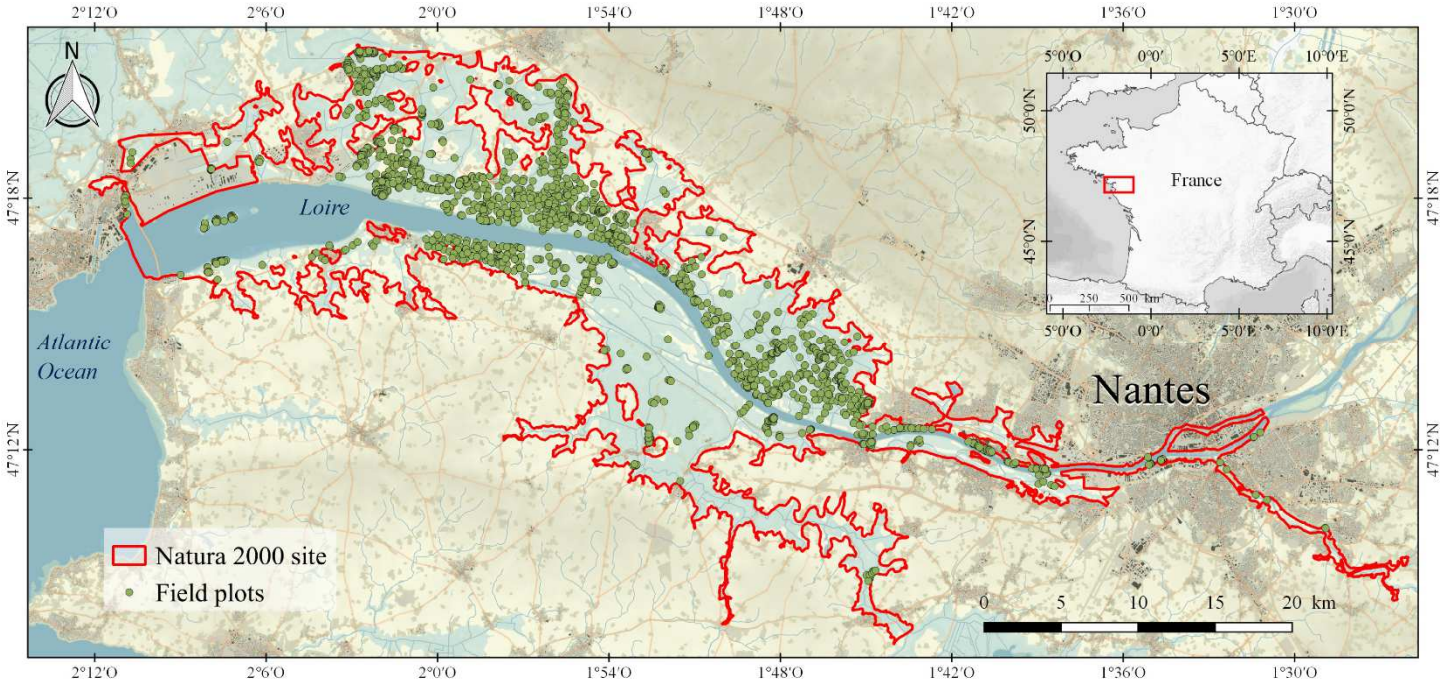

Fig. 1. Location of the Natura 2000 site 'Estuaire de la Loire' and available ground data.

2.2 Typology of habitat types

We used two habitat classification systems to establish the typology: EUNIS (European Union Nature Information System), which represents the most complete habitat repository in Europe, covering both marine and terrestrial environments (Chytrý et al., 2020; Evans, 2012) and the Interpretation Manual of European Union Habitats-EUR28 (European Commission, 2013), which includes definitions of the habitats of community interest in annex 1 of HabDir.

The typological units of these habitat repositories are mostly defined by vegetation classifications derived from sigmatist phytosociology (Gayet et al., 2018; Rodwell et al., 2018). We established the study site's habitat typology by identifying field vegetation plots which were collected using the sigmatist phytosociological method. A vegetation plot corresponds to the list of plant species inventoried inside areas with a floristically homogeneous composition (Dengler et al. 2008). The cover

of each species is visually estimated and quantified according to the Braun-Blanquet's scale (Braun-Blanquet, 1932).

We used 1,248 phytosociological vegetation plots to obtain a representative sampling of the diversity of habitat types present in the study site (Fig. 1). A total of 989 phytosociological vegetation plots were collected from the bibliography (scientific publications, PhD theses, impact studies, vegetation maps…) and we collected in the field 259 phytosociological vegetation plots for this study. This dataset is constituted of vegetation plots that were collected from 2010 to 2019. Older vegetation plots were not selected because of a too long-time gap between field and satellite data. Most bibliographical vegetation plots were located precisely (horizontal accuracy <5 m) and those collected during this study were georeferenced using a differential GPS (GPS GeoXH™ from Trimble Geo-Explorer®, horizontal accuracy <1 m).

Firstly, we assigned vegetation plots to a phytosociological unit based on the descriptions contained in the Prodrome of French Vegetation (Bioret et al., 2013). Secondly, phytosociological units were related to EUNIS and EUR28 habitat types. This step (hereafter call "crosswalks") has been carried out using the French repository of habitats and vegetation typologies HABREF (Clair et al., 2019).

2.3 Acquisition of Sentinel-2 images

Covering the entire site requires using two Sentinel-2 image tiles (tiles' identification numbers: T30TWT and T30TXT). We looked for images without cloud cover and regularly distributed along an annual cycle of vegetation. Overall, we used 22 Sentinel-2 images (Level-2A – product-Bottom of Atmosphere (BOA) reflectance), corresponding to 11 acquisition dates from autumn 2018 to summer 2019 (Fig. 2).

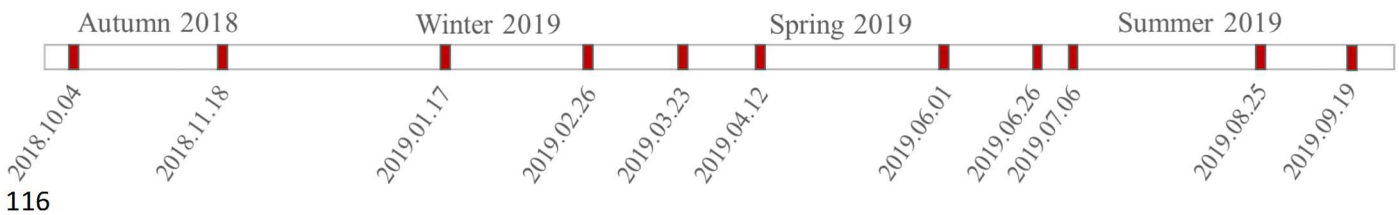

Fig. 2. Acquisition dates of Sentinel-2 images during an annual cycle of vegetation.

2.4 Image preparation and vegetation indices calculations

Sentinel-2 images are distributed with three spectral bands at 60m spatial resolution (B1, B9 and B10), six bands at 20m spatial resolution (B5, B6, B7, B8A, B11 and B12) and four bands at 10m spatial resolution (B2, B3, B4 and B8) (Table 1). For each date, we only selected the bands with a spatial resolution of 10m and 20m (the 60m bands were mostly intended for the atmospheric corrections). We stacked the bands with the same spatial resolution and the 20m bands were interpolated on a 10m grid using the bilinear approach. Finally, all bands were stacked to form an image of 10 spectral bands with a 10-meter spatial resolution.

Table 1 Sentinel-2 band characteristics

Sentinel-2 bands	Spectral region	Central wavelength (nm)	Bandwidth (nm)	Resolution (m)
B1	Coastal aerosol	442.7	21	60
B2	Blue	492.4	66	10
B3	Green	559.8	36	10
B4	Red	664.6	31	10
B5	Red-edge 1	704.1	15	20
B6	Red-edge 2	740.5	15	20
B7	Red-edge 3	782.8	20	20
B8	Near-infrared	832.8	106	10
B8A	Near-infrared narrow	864.7	21	20
B9	Water vapour	945.1	20	60
B10	Shortwave-infrared - Cirrus	1373.5	31	60
B11	Shortwave-infrared 1	1613.7	91	20
B12	Shortwave-infrared 2	2202.4	175	20

Calculating vegetation indices

Remote sensing spectral indices are based on the combination of spectral bands to highlight biophysical characteristics of land surfaces. They are particularly useful for multi-date classifications as they are good indicators of seasonal changes of vegetation cover (Schuster et al., 2015). In this study, we have selected a set of 12 spectral indices (Table 2) covering the full spectral domain of

Sentinel-2 and commonly used for vegetation mapping (Adam et al., 2010; Kaplan and Avdan, 2017; Roberts et al., 2011; Wakulińska and Marcinkowska-Ochtyra, 2020). NDVI remains the most commonly used index with a very sensitive response to green vegetation thanks to its pigment absorption ratio in the red range of electromagnetic spectrum and cell reflectance in the near-infrared range (NIR), but it remains sensitive to effects of soil color, soil brightness and atmospheric effects. GNDVI differs from NDVI by establishing a ratio between the NIR and the green range. SAVI considers the effects of the soil more, which theoretically improves NDVI while EVI focuses more on atmospheric effects. The red-edge curve is more specifically targeted with MCARI. NDWI targets leave with the NIR and shortwave-infrared (SWIR) ratio sensitive to water content in leaves. Each index is therefore part of the overall answer to the problem of identifying habitat types, answer given by the combination of these indices. They are then stacked with the ten retained Sentinel-2 spectral bands to provide a file with 22 layers (12 indices and 10 spectral bands) for each date.

Table 2 List of vegetation indices calculated using Sentinel-2 spectral bands.

Vegetation index	Formulation	Sentinel-2 bands used	References
NDVI	(NIR - R) / (NIR + R)	(B8 - B4) / (B8 + B4)	*Rouse et al., 1973*
NDWI	(NIR - SWIR1) / (NIR + SWIR1)	(B8 - B11) / (B8 + B11)	*Gao, 1996*
GNDVI	(NIR - G) / (NIR + G)	(B8 - B3) / (B8 + B3)	*Gitelson et al., 1996*
IReCI	(NIR - R) / (RE1 / RE2)	(B8 - B4) * (B5 / B6)	*Frampton et al., 2013*
PSSRa	NIR / R	B8 / B4	*Blackburn, 1998*
NDI45	(RE1 - R) / (RE1 + R)	(B5 - B4) / (B5 + B4)	*Delegido et al., 2011*
EVI	2.5 * (NIR - R) / ((NIR + 6* R - 7.5 * B) + 1)	2.5 * (B8 - B4) / ((B8 + 6 * B4 - 7.5 * B2) + 1)	*Huete et al., 2002*
SAVI	((NIR - R) / (NIR + R + 0.428)) * (1 + 0.428)	(B8 - B4) / (B8 + B4 + 0.428) * (1.0 + 0.428)	*Huete, 1988*
MCARI	[(RE1 - R) - 0.2 (RE1 - G)] * (RE1 - R)	((B5 - B4) - 0.2 * (B5 - B3)) * (B5 / B4)	*Daughtry et al., 2000*
CRE	((NIR / RE1) - 1.0)	((B8 / B5) - 1.0)	*Gitelson et al., 2006*
S2REP	705 + 35 * ((((NIR + R) / 2) - RE1) / (RE2 - RE1))	705 + 35 * ((((B8 + B4) / 2) - B5) / (B6 - B5))	*Frampton et al., 2013*
MTCI	(RE2 - RE1) / (RE1 - R)	(B6 - B5) / (B5 - B4)	*Dash and Curran, 2004*

B, G, R, RE1, RE2, NIR, SWIR1, represent blue, green, red, red-edge 1, red-edge 2, near-infrared and and shortwave-infrared 1 spectral bands.

NDVI: Normalised Difference Vegetation Index
NDWI: Normalized Difference Water Index
GNDVI: Green Normalised Difference Vegetation Index
IReCI: Inverted Red-Edge Chlorophyll Index
PSSRa: Pigment Specific Simple Ratio
NDI45: Normalized difference index 4 and 5
EVI: Enhanced Vegetation Index
SAVI: Soil Adjusted Vegetation Index
MCARI: Modified chlorophyll absorption in reflectance index
CRE: Chlorophyll Red-Edge index
S2REP: Sentinel-2 red-edge position
MTCI: MERIS Terrestrial Chlorophyll Index

1.

Finally, we cropped the images according to the study area's limits and we excluded artificial areas using auxiliary thematic layers integrating roads, built-up and cultivated areas as suggested by Inglada et al. (2017) and Rapinel et al. (2015).

153 *2.5 Selection of training data*

154 We vectorized a Sentinel-2 image to build a vector grid consisting of 100m2 polygons (10*10m) used
155 as support to select training areas. We superimposed this grid on a very high spatial resolution image
156 from spring 2018 (Google Earth: Images CNES ©/Airbus, Maxar Technologies©). Based on the
157 location of the phytosociological vegetation plots, we individually and manually selected polygons
158 covering visually homogenous vegetation units ('pure' pixels) (Fig. 3). The training areas had to
159 respect a criterion of physiognomic and colorimetric homogeneity so as not to select mixed habitats
160 (mosaic) or pixels overlapping several typological units.

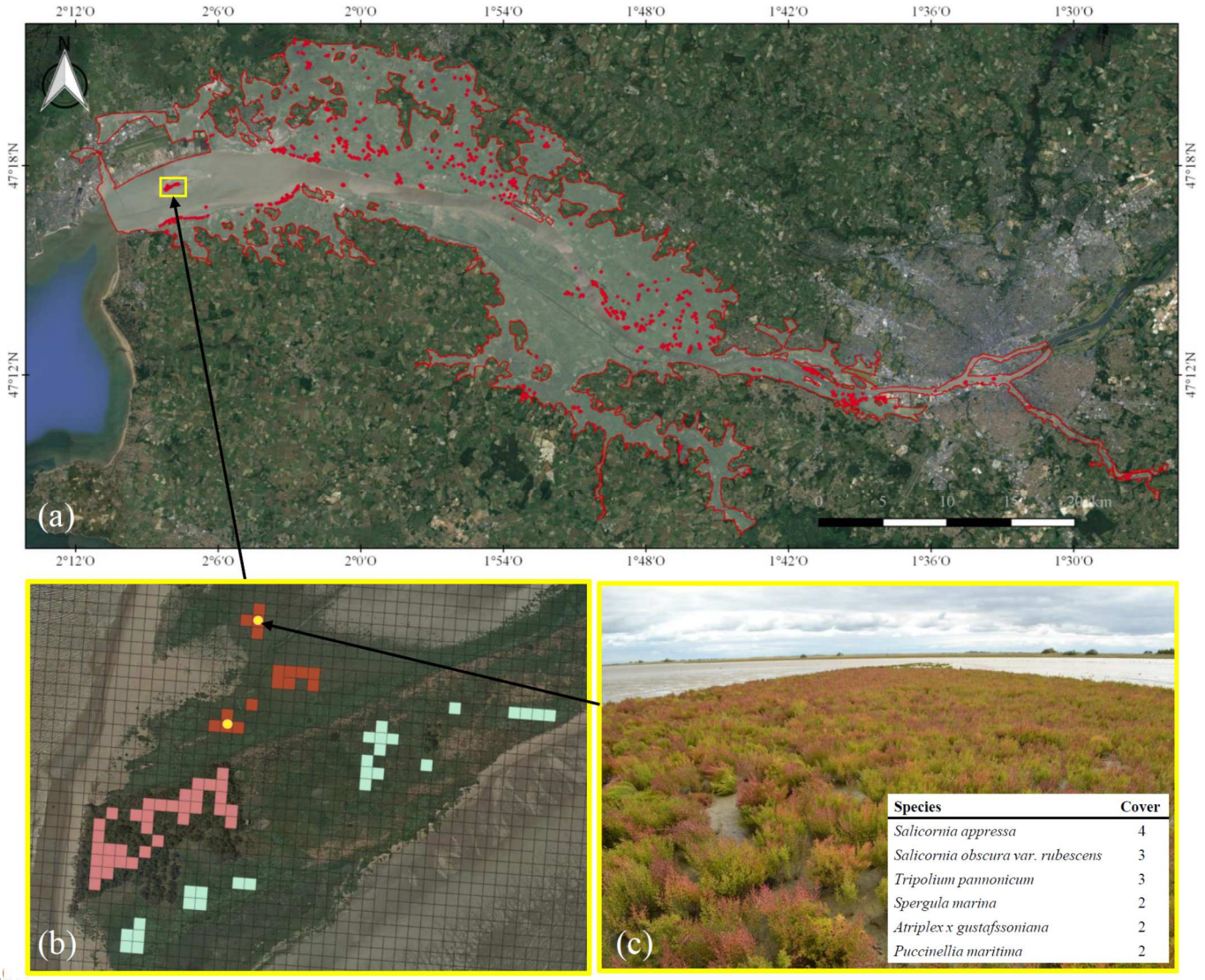

162 **Fig. 3.** Methodological process to select training data. (a) very high spatial resolution image of the
163 study area (the red marked pixels indicate the training data's location). (b) Zoom on a part of the study

area with the vector grid displayed and the polygons selected for three EUNIS habitats (red: EUNIS A2.551; pink: EUNIS F9.3131; sea green: EUNIS A2.511). The yellow dots correspond to the phytosociological vegetation plot locations. (c) A phytosociological vegetation plot and photograph of habitat EUNIS A2.551 acquired during fieldwork.

We used a study of the spatio-temporal dynamics of vegetation in the Loire estuary (Le Dez et al., 2017) to determine the level of stability of plant communities in the study area. For plant communities with a high degree of stability (e.g. woodlands, forests and some types of meadows), we selected training areas using data up to the year 2010. On the other hand, for highly dynamic plant communities, we have only kept the plots collected during the year of acquisition of satellite images (e.g. annual salt marshes vegetation (A2.551 – '*Salicornia*, *Suaeda* and *Salsola* pioneer salt marshes') or reedbeds on regularly submerged banks (C3.27 – 'Halophile *Scirpus*, *Bolboschoenus* and *Schoenoplectus* beds'). In addition, during the pixel selection phase by photo-interpretation, we checked that the pixels viewed and the habitat categories identified in the typology were consistent so as not to take training samples in locations where the vegetation might have changed.

Finally, we selected additional pixels for some habitat categories that were easily recognizable by photo-interpretation and for which we had little field data (e.g. C3.21 – '*Phragmites australis* beds' or G1.1111 – 'Western European white willow forests').

We made sure to select a number of training data that was proportional to the area covered by each habitat on the study site (Colditz 2015; Raab et al., 2018).

2.6 Classification method

2.6.1 Choosing the classification algorithm

We used the Random Forest (RF) algorithm (Breiman 2001) to classify the habitats. RF is a machine learning classifier commonly used in remote sensing and many studies showed that it could produce accurate maps of vegetation and habitats types, including from Sentinel-2 (Marzialetti et al., 2019;

189 Rapinel et al., 2020; Wittke et al., 2019). RF is especially known to be fast (requiring little calculation
190 effort) and able to process asymmetric data with many predictive variables (Millard and Richardson,
191 2015; Sławik et al., 2019). In RF model, the original training data are randomly sampled-with-
192 replacement generating bootstrap samples. Each decision tree in RF is trained on an 'in bag' sample of
193 the original training data. The remaining sample ('out of bag' sample) is used to be predicted by all the
194 decision trees that allowed to evaluate the outcome (known as OOB score). For our analyses, we set
195 the number of trees to 2,000 and the number of randomly sampled variables as candidates for each
196 split to six.

197 We used the overall accuracy index (OA) and the Kappa coefficient to evaluate the overall quality of
198 classification models (Smits et al., 1999; Stehman, 1997). We produced confusion matrices
199 representing errors by class after each modeling and we calculated the producer's, as well as the user's
200 accuracy (respectively PA and UA), for each habitat (Congalton, 1991). These accuracy assessment
201 metrics are commonly used in remote sensing (Belgiu and Csillik, 2018; Calleja et al., 2019; Rana and
202 Venkata Suryanarayana, 2020). After processing each image, we applied the model produced from the
203 training areas to the entire image to create a predictive habitat classification of the entire study area.

204

205 *2.6.2 Selection of the most important variables for multi-date image classification*

206 From the 11 Sentinel-2 image acquisition dates, we identified the most important variables
207 (acquisition dates, spectral bands and vegetation indices) to classify habitats of the Natura 2000 site. It
208 is possible to select the best variables using automatized methods as suggested by the Recursive
209 Feature Elimination algorithm (Radecka et al., 2019; Rapinel et al., 2019). However, we chose to
210 develop our supervised methodology by first assessing which of the 11 image acquisitions were
211 relevant for separating habitat classes. The general objective is to first integrate seasonal phenological
212 variations for all the habitats in the study site. Vegetation growth stages differ among plant
213 communities which is an important characteristic to be used for classification. Thus, the images must

include vegetation changes starting with the development of the earliest plant communities until those appearing the latest (mainly from early spring to autumn for this site).

First, we performed an RF classification for each of the 11 dates and we assessed the overall quality of the classification models using OA. We wanted to only keep the acquisition dates of the images with the highest performance, so we set an accuracy threshold at 80% (OA=0.8). Above this percentage, we considered the classification result as satisfying, as suggested by Rapinel et al. (2014) and Zlinszky et al. (2014). All images over this threshold (OA>0.8) were retained while those below (OA<0.8) were excluded because we considered their performance as too low.

Secondly, we tested the importance of the spectral variables (spectral bands and vegetation indices) using the measures of mean decrease Gini (MDG) obtained from the RF algorithm classification (Hubert-Moy et al., 2020; Li et al., 2019). For each selected date (OA>80%), we selected the five best performing variables (spectral bands, vegetation indices) based on MDG (Grabska et al., 2019). Finally, we stacked all these variables (five best performing bands and/or indices of the dates with OA>80%) to build the multi-date feature dataset.

2.7 Software:

We used the R software (version 3.6.2) (R Development Core Team, 2019) for our analyses, with the packages 'randomForest' (version 4.6-14) (Liaw & Wiener, 2002), 'rgdal' (version 1.4-8) (Bivand et al., 2015) and 'raster' (version 3.0-7) (Hijmans, 2015). The results were visualized in QGIS 3.4.8 (QGIS Development Team, 2019).

3. Results

3.1. Typology of habitats

238 *3.1.1. Complete typology of habitats in the Natura 2000 site*

239 The complete typology brings together all the habitats identified on the study site. They are presented
240 in Appendix A. Overall, we characterized 74 phytosociological units based on phytosociological plots'
241 identification.

242 The crosswalk of phytosociological units with EUNIS habitat types led us to identify 62 habitats.
243 Waterbodies and reed bed habitats and grassland habitats were the most diversified with 19 and 15
244 habitats respectively. Two grassland habitats are made of a mosaic of EUNIS habitats (E2.1xE2.5 &
245 E3.44xA2.5) linked to vegetation plots with an intermediate floristic composition between several
246 vegetation communities (transitional vegetation). Marine habitats are also diversified with 14 EUNIS
247 habitats inventoried. Woodland and forest habitats, as well as shrubs and thicket habitats are more
248 unified with respectively 7 and 6 EUNIS habitats. Finally, cultivated plots constitute the last EUNIS
249 habitat in our typology.

250 The crosswalk with EUR28 habitat types led us to determine 15 habitats of community interest (HCI)
251 including 3 that are considered as a priority. All the marine habitats are HCIs and represent half of the
252 total number of HCIs with 7 EUR28 habitats, including 1 priority. The other HCIs include waterbodies
253 and reed bed habitats (4 HCIs, of which 1 is a priority), grassland habitats (2 HCIs), woodland and
254 forest habitats (2 HCIs, of which 1 is a priority) and shrub and thicket habitats (1 HCI).

255

256 *3.1.2. Typology retained for the classifications after selection of the training data*

257 The typology retained to classify the images is presented in Table 3. It includes all phytosociological
258 units for which training areas could be selected. The other phytosociological units did not cover
259 enough surface area to compose 'pure' pixels; therefore, they could not be integrated into this
260 typology.

Ultimately, only 44 of the 74 phytosociological units identified could be included in the final typology. This result corresponds to 39 EUNIS habitats out of the 62 identified and 9 EUR28 habitats out of the 15 identified in the Natura 2000 site.

Table 3 Habitat typology used for image classification (habitats for which pixels could be selected). 'Nb pixels' corresponds to the number of pixels selected as training area for the image classification. The EUR28 habitats marked in bold correspond to priority habitats of community interest in HabDir. Fields marked with an asterisk correspond to non-vegetated or artificialized areas. They were assigned to habitat typologies based on the biotope using the criteria of the French EUNIS habitat determination guide (Gayet et al., 2018) and the 'Cahiers d'habitats' (Bensettiti et al., 2001–2005).

Physiognomic units	Phytosociological units	Nb pixels	EUNIS habitats	EUR 28 habitats
Marine habitats	*Sandy shore comprising clean sands (coarse, medium or fine-grained) and muddy sands	47	A2.2 - Littoral sand and muddy sand	1130 - Estuaries
	*Muddy shores of fine particulate sediment, mostly in the silt and clay fraction	195	A2.3 - Littoral mud	
	Thero – Salicornietalia dolichostachyae Tüxen *ex* Boullet & Géhu 2004	92	A2.551 - *Salicornia* , *Suaeda* and *Salsola* pioneer saltmarshes	1310 - *Salicornia* and other annuals colonising mud and sand
	Parapholido strigosae – Hordeetum marini (Géhu et al. 1975) Géhu & de Foucault 1978	66	A2.553 - Atlantic *Sagina maritima* communities	
	Puccinellietum maritimae Christiansen 1927	92	A2.542 - Atlantic lower shore communities	1330 - Atlantic salt meadows (*Glauco-Puccinellietalia maritimae*)
	Glauco maritimi – Juncion maritimi Géhu & Géhu-Franck *ex* Géhu in Bardat et al. 2004	21	A2.531 - Atlantic upper shore communities	
	Agropyrion pungentis Géhu 1968	152	A2.511 - Atlantic saltmarsh and drift rough grass communities	
	Alopecurion utriculati Zeidler 1954	777	A2.523 - Mediterranean short *Juncus* , *Carex* , *Hordeum* and *Trifolium* saltmeadows	1410 - Mediterranean salt meadows (*Juncetalia maritimi*)
	Ranunculo ophioglossifolii – Oenanthion fistulosae de Foucault in de Foucault & Catteau 2012	97		
Waterbodies and reedbeds habitats	*Open fresh or brackish waterbodies	96	C - Inland surface waters	
	*Loire river subject to the tid	125	X01 - Estuaries	
	Glycerietum fluitantis Nowiński 1930	119	C3.1 - Species-rich helophyte beds	
	Phragmitetum communis Savič 1926 and *Astero tripolii – Phragmitetum communis* Jeschke *ex* Krisch 1974	390	C3.21 - *Phragmites australis* beds	
	Glycerietum aquaticae Nowiński 1930	307	C3.251 - Sweetgrass beds	
	Scirpion maritimi Dahl & Hadač 1941	185	C3.27 - Halophile *Scirpus* , *Bolboschoenus* and *Schoenoplectus* beds	
	*Mud bottoms of waterbodies	15	C3.6 - Unvegetated or sparsely vegetated shores with soft or mobile sediments	
	Galio palustris – Caricetum rapariae Bal.-Tul., Mucina, Ellmauer & B.Walln. in G.Grabherr & Mucina 1993	48	D5.21 - Beds of large *Carex spp.*	
Grasslands habitats	*Thero – Airion* Tüxen ex Oberdorfer 1957	113	E1.91 - Dwarf annual siliceous grassland	
	Mesophile hay meadows (*Cynosurion cristati* Tüxen 1947; *Lolio perennis – Plantaginion majoris* G. Sissingh 1969)	311	E2.1 - Permanent mesotrophic pastures and aftermath-grazed meadows	
	Cynosurion cristati Tüxen 1947 X Grp des *Sisymbrietea officinalis*	81	E2.1 - Permanent mesotrophic pastures and aftermath-grazed meadows X E5.1 - Anthropogenic herb stands	
	*Land occupied by heavily fertilised or reseeded permanent grasslands	45	E2.6 - Agriculturally-improved, re-seeded and heavily fertilised grassland, including sports fields and grass lawns	
	Oenanthion fistulosae de Foucault 2008	141	E3.41 - Atlantic and sub-Atlantic humid meadows	
	Bromion racemosi Tüxen ex de Foucault 2008	246		
	Ranunculo repentis – Cynosurion cristati Passarge 1969	46		
	Wet and humid meadows dominated by *Juncus effusus*	23	E3.417 - Soft rush meadows	
	Hygrophilic pastures regularly flooded by the oligohaline water of Loire River and dominated by *Agrostis stolonifera*	125	E3.44 - Flood swards and related communities	
	Meso-hygrophilic pastures regularly flooded by the oligohaline water of Loire River and dominated by *Agrostis stolonifera*	121		
	Pastures regularly flooded by the oligohaline water of Loire River and dominated by *Juncus inflexus*	101	E3.441 - Tall rush pastures	
	Hygrophilic pastures regularly flooded by the brackish water of Loire River and dominated by *Agrostis stolonifera*	113	E3.44 - Flood swards and related communities X A2.5 - Coastal saltmarshes and saline reedbeds	
	Meso-hygrophilic pastures regularly flooded by the brackish water of Loire River and dominated by *Agrostis stolonifera*	41		
	Juncion acutiflori Braun-Blanquet in Braun-Blanquet & Tüxen 1952	20	E3.512 - Acidocline purple moorgrass meadows	6410 - *Molinia* meadows on calcareous, peaty or clayey-siltladen soils (*Molinion caeruleae*)
	Sisymbrietea officinalis Korneck 1974 and *Convolvulo arvensis – Agropyrion repentis* Görs 1966	33	E5.1 - Anthropogenic herb stands	
	Achilleo ptarmicae – Cirsion palustris Julve & Gillet ex de Foucault 2011	19	E5.412 - Western nemoral river bank tall-herb communities dominated by *Filipendula*	6430 - Hydrophilous tall herb fringe communities of plains and of the montane to alpine levels
Scrubs and thickets habitats	*Solano dulcamarae – Tamaricetum gallicae* de Foucault 2008	34	F9.3131 - West Mediterranean tamarisk thickets	92D0 - Southern riparian galleries and thickets (*Nerio - Tamaricetea* and *Securinegion tinctoriae*)
	Species-poor *Prunus spinosa* or *Rubus spp.* thickets	91	F3.111 - Blackthorn-bramble scrub	
	Salicetum triandro – viminalis (Tüxen 1931) Lohmeyer 1952 *ex* Moor 1958	174	F9.121 - lmond willow-osier scrub	
	Low woods and scrubs dominated by *Salix atrocinerea*	68	F9.2 - *Salix* carr and fen scrub	
Woodland and forest habitats	*Salicion albae* Soó 1930	134	G1.1111 - Western European white willow forests	**91E0 - Alluvial forests with *Alnus glutinosa* and *Fraxinus excelsior* (*Alno-Padion* , *Alnion incanae* , *Salicion albae*)**
	Alnenion glutinoso - incanae Oberdorfer 1953	23	G1.211 - *Fraxinus - Alnus* woods of rivulets and springs	
	Ulmo laevis – Fraxinetum angustifoliae (Breton) Rameau & Schmitt ex J.-M. Royer, Felzines, Misset & Thévenin 2006	89	G1.22 - Mixed *Quercus - Ulmus - Fraxinus* woodland of great rivers	91F0 - Riparian mixed forests of *Quercus robur* , *Ulmus laevis* and *Ulmus minor* , *Fraxinus excelsior* or *Fraxinus angustifolia* , along the great rivers (*Ulmenion minoris*)
	Meso-hygrophilic forests dominated by *Quercus robur* and *Fraxino excelsioris – Quercion roboris* Rameau 1996	269	G1.A1 - *Quercus - Fraxinus - Carpinus* betulus woodland on eutrophic and mesotrophic soils	
	Plantations of species, hybrids or cultivars of the deciduous genus *Populus*	136	G1.C1 - *Populus* plantations	
	Plantations of Palaearctic conifers of genus *Pinus*	113	G3.F12 - Native pine plantations	
Cultived agricultural habitats	Cereal crops	65	I1.1 - Intensive unmixed crops	

271

272 The number of training pixels per typological unit varies from 15 (mud bottoms of waterbodies) to 777
273 (*Alopecurion utriculati* Zeidler 1954). Overall, 5,564 training pixels were selected for all the data.

274

275 *3.2 Analyses of single date images*

276 Overall accuracy indices of the single classification of the Sentinel-2 images for the 11 selected dates
277 are presented in Fig. 4. Images acquired during spring and summer gave the best results (OA>85%).

The highest accuracy was obtained with the image of July 6, 2019 (OA=87.28%). The classifications of the images taken at the end of winter and in autumn present slightly lower results (80 %< OA <85%). The less accurate classifications are from the late autumn and winter images (OA <80%).

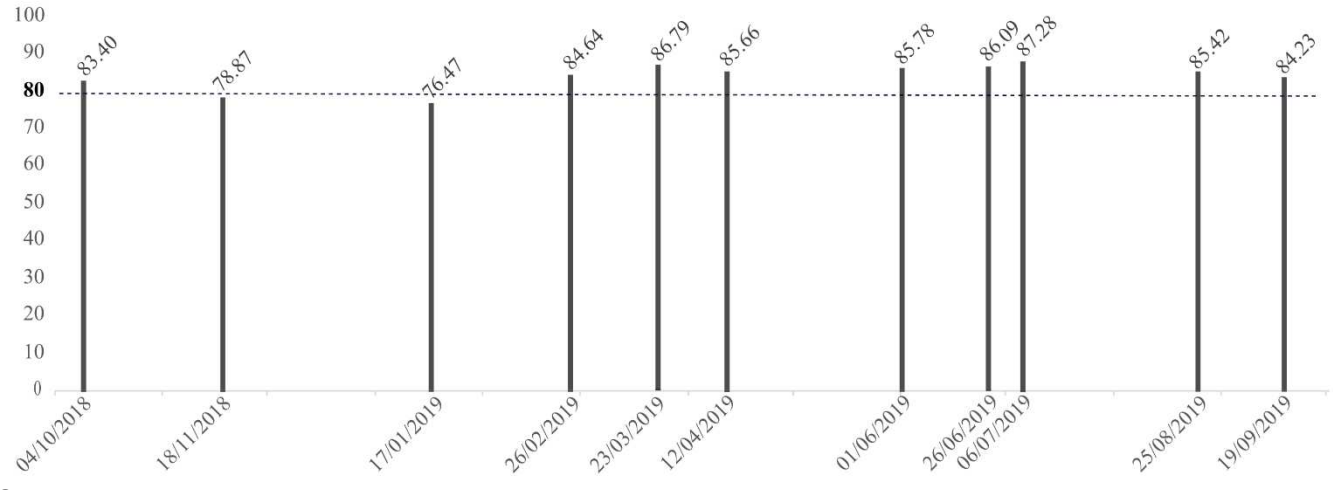

Fig. 4. Overall accuracy indices of the single date classifications of Sentinel-2 images for the 11 dates. The dotted line shows the 80% threshold used to select the best-performing dates.

3.3 Selected variables to build the multi-date feature dataset

Based on the results of the single-image classifications, we selected images of nine dates that had an overall accuracy higher than 80% (Fig. 4). For each of these dates, we kept the five variables (spectral bands and vegetation indices) that contribute most to the classification result according to MDG (Table 4, Appendix B). In total, six different spectral bands and four vegetation indices were included in the multi-date feature dataset. The spectral bands B11 and B12 (SWIR) were systematically present for the nine dates, while the bands B5 (red-edge), B3 (green) and B2 (blue) are only present for six, four and two dates respectively and the band B8A (near-infrared narrow) only for one date. Regarding vegetation indices, GNDVI and MTCI are present for seven and four dates respectively, whereas NDWI and EVI both appear for two dates. In total, 45 variables were retained and stacked to build the multi-date feature dataset.

Table 4 List of the five variables that contributed most to the single-date image classification (spectral bands and vegetation indices) according to MDG for each date. The number indicates the variable's order of importance according to MDG for each date (the most contributing variables are indicated by the lowest numbers - for more details, see Appendix B).

	20181004	20190226	20190323	20190412	20190601	20190626	20190706	20190825	20190919
B11	1	2	2	1	1	1	1	1	1
B12	2	1	1	2	2	3	2	2	2
B5		3	3		4	2	3	3	
GNDVI	5	5	4	4			5	5	5
MTCI		4		3	3	5			
B3	4		5	5					4
NDWI	3								3
B2						4		4	
EVI							4		
B8A					5				

Fig. 5 shows the seasonal variations of the main variables (Table 4) for habitat discrimination. The GNDVI index and B2 (blue) and B3 (green) spectral bands allow good discrimination of habitats A2.2 'Littoral sand and muddy sand' and A2.3 – 'Littoral mud' all year long. On the contrary, the phenological profiles of the other habitats cannot be easily distinguished over the period studied. Overall, temporal profiles have more similar values during wintertime. The main reflectance and intensity variations of the indices are observed in spring and summer. More precisely, it is the temporal shifts in spectral responses that allow the distinction of habitats. For example, habitats A2.523 – 'Mediterranean short *Juncus, Carex, Hordeum* and *Trifolium* salt meadows' and A2.511 – 'Atlantic salt marsh and drift rough grass communities' show similar profiles on some bands (B11 and B12) and some indices (NDWI and EVI). However, they peak at different dates (June 26, 2019, for A2.523 and August 25, 2019, for A2.51) because of mowing taking place at different times.

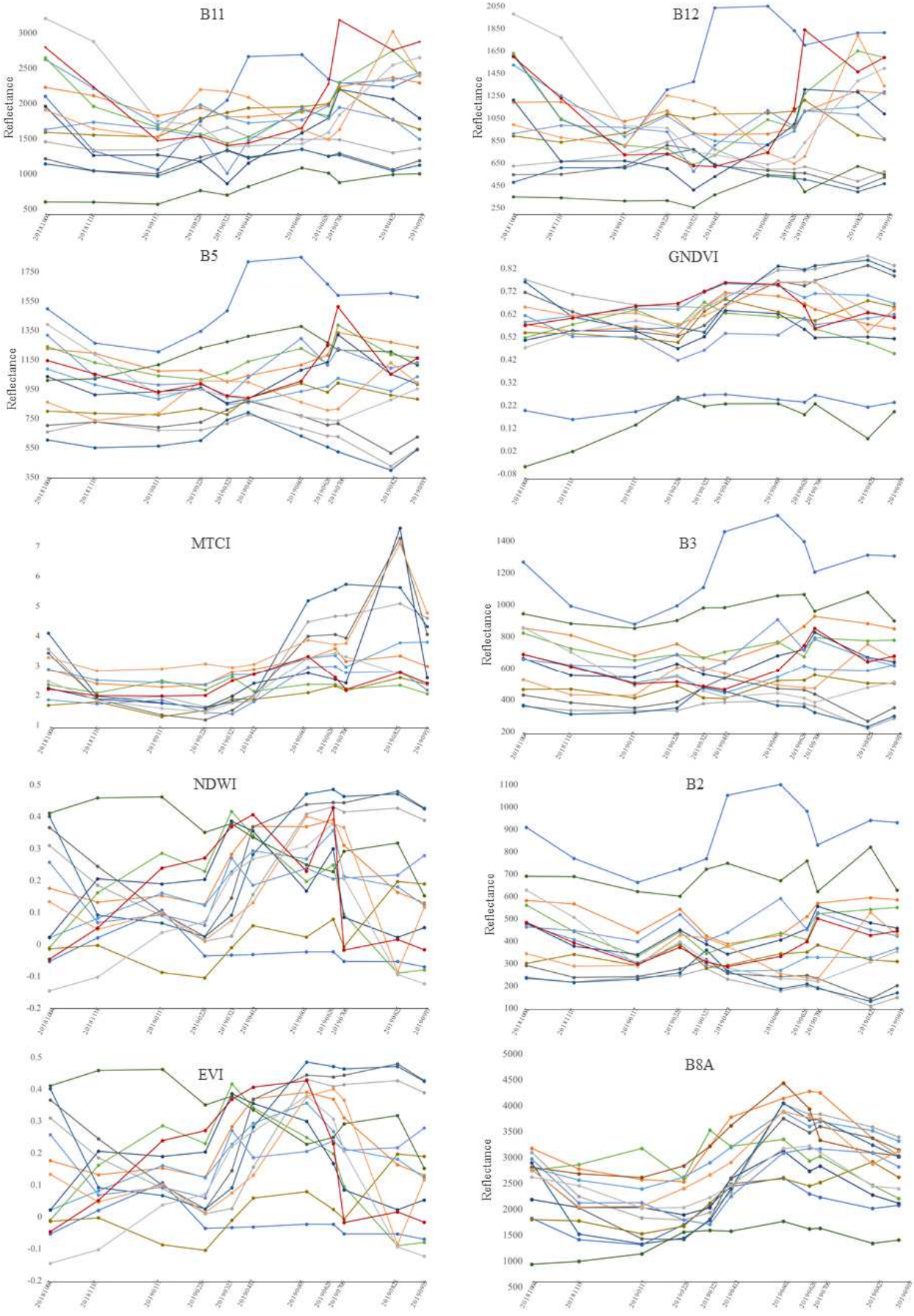
B11
B12
B5
GNDVI
MTCI
B3
NDWI
B2
EVI
B8A
Reflectance
A2.2
A2.511
G1.211
E3.512
A2.553
A2.542
G1.1111
F9.3131
G1.22
A2.3
A2.551
E5.412
A2.531
A2.523

316 **Fig. 5.** Seasonal variations of the most important variables (Table 4) for habitat discrimination in the
317 study site. Only the spectral profiles of EUNIS habitats characterizing habitats of community interest
318 are represented. The curves are plotted from the average for all training pixels for each habitat.

319

320 *3.4 Multi-date classification*

321 The confusion matrix showing the results of the RF classification of the multi-date feature dataset is
322 presented in Table 5. The predictive habitat map obtained after running the RF model on all pixels of
323 the investigation area is shown in Fig. 6. The results are presented at the EUNIS habitats level after
324 merging the phytosociological units corresponding to the same habitat category, following the
325 crosswalks in Table 3.

326 The overall evaluation of the model shows highly satisfying results with an overall accuracy of 98.7%
327 and a kappa coefficient of 0.99. The producer's accuracy is 100% for 19 habitats out of the 39 in the
328 EUNIS habitat typology. The other habitats present moderate errors leading us to obtain a producer's
329 accuracy higher than 90%, except for EUNIS habitats D5.21, E3.512 and F9.2 with a PA of 87.5%,
330 75% and 89.7% respectively. These results indicate that these habitats tend to be underrepresented in
331 the predicted habitat map (Fig. 6).

332 In the same way, the user's accuracy is highly satisfying with 21 habitats with 100% UA whereas
333 other habitats still present an accuracy higher than 90% UA. These slight confusions lead to an
334 overrepresentation of habitats in the predicted map (Fig. 6).

335 Figure 7 shows that habitats with a high number of training areas obtain a very high estimated
336 producer's accuracy (PA). This is the case for habitat A2.523 – 'Mediterranean short *Juncus, Carex,*
337 *Hordeum* and *Trifolium* salt meadows' with 874 training pixels and a 99.4% PA or habitat E3.41 –
338 'Atlantic and sub-Atlantic humid meadows' with 706 pixels and a 99.6% PA. Conversely, habitats
339 with a lower PA have fewer training areas, such as habitat E3.512 – 'Acidocline purple moor grass
340 meadows' with 20 training and a 75% PA or habitat D5.21 – 'Beds of large *Carex spp.*' with 48

training pixels and an 87.5% PA. However, some habitats with few training areas are very well modeled due to their specific spectral signatures, which are very different from those of other habitats. This is the case for habitats A2.531 – 'Atlantic upper shore communities' (21 pixels and a 100% PA) or E5.412 – 'Western nemoral river bank tall-herb communities dominated by *Filipendula*' (19 pixels and a 100% PA).

Table 5 Confusion matrix between the reference data (line) and the classified data by RF (columns) for the 39 EUNIS habitats.

Classified data

Reference data: EUNIS Code	A2.2	A2.3	A2.551	A2.553	A2.531	A2.542	A2.511	A2.523	C	X01	C3.1	C3.21	C3.251	C3.27	C3.6	D5.21	E1.91	E2.1	E2.1 X A5.1	E2.6	E3.41	E3.417	E3.44	E3.44 X A2.5	E3.441	E3.512	E5.1	E5.412	F3.111	F9.121	F9.2	F9.3131	G1.1111	G1.211	G1.22	G1.A1	G1.C1	G3.F12	I1.1	Producer's accuracy (%)
A2.2	47	.	.	.	.	.	.	.	.	.	.	.	.	.	.	.	.	.	.	.	.	.	.	.	.	.	.	.	.	.	.	.	.	.	.	.	.	.	.	.	100
A2.3	.	195	.	.	.	.	.	.	.	.	.	.	.	.	.	.	.	.	.	.	.	.	.	.	.	.	.	.	.	.	.	.	.	.	.	.	.	.	.	.	100
A2.551	.	.	92	.	.	.	.	.	.	.	.	.	.	.	.	.	.	.	.	.	.	.	.	.	.	.	.	.	.	.	.	.	.	.	.	.	.	.	.	.	100
A2.553	.	.	.	66	.	.	.	.	.	.	.	.	.	.	.	.	.	.	.	.	.	.	.	.	.	.	.	.	.	.	.	.	.	.	.	.	.	.	.	.	100
A2.531	.	.	.	.	21	.	.	.	.	.	.	.	.	.	.	.	.	.	.	.	.	.	.	.	.	.	.	.	.	.	.	.	.	.	.	.	.	.	.	.	100
A2.542	.	.	.	1	.	88	.	.	.	.	.	.	.	.	.	.	.	.	.	.	.	1	2	.	.	.	.	.	.	.	.	.	.	.	.	.	.	.	.	.	95.7
A2.511	.	.	.	.	.	.	150	.	.	.	.	.	.	.	.	.	.	.	.	.	1	.	1	.	.	.	.	.	.	.	.	.	.	.	.	.	.	.	.	.	98.7
A2.523	.	.	.	.	.	.	.	869	.	.	.	.	.	.	.	.	.	.	.	.	3	.	2	.	.	.	.	.	.	.	.	.	.	.	.	.	.	.	.	.	99.4
C	.	.	.	.	.	.	.	.	96	.	.	.	.	.	.	.	.	.	.	.	.	.	.	.	.	.	.	.	.	.	.	.	.	.	.	.	.	.	.	.	100
X01	.	.	.	.	.	.	.	.	.	125	.	.	.	.	.	.	.	.	.	.	.	.	.	.	.	.	.	.	.	.	.	.	.	.	.	.	.	.	.	.	100
C3.1	.	.	.	.	.	.	.	.	.	.	118	.	.	.	.	.	.	.	.	.	.	.	1	.	.	.	.	.	.	.	.	.	.	.	.	.	.	.	.	.	99.2
C3.21	.	.	.	.	.	.	.	1	.	.	.	386	.	1	.	.	.	.	.	.	1	.	.	.	.	.	.	.	.	1	.	.	.	.	.	.	.	.	.	.	99.0
C3.251	.	.	.	.	.	.	.	.	.	.	.	.	307	.	.	.	.	.	.	.	.	.	.	.	.	.	.	.	.	.	.	.	.	.	.	.	.	.	.	.	100.0
C3.27	.	.	.	.	.	.	.	.	.	.	.	1	.	182	.	.	.	.	.	.	1	.	1	.	.	.	.	.	.	.	.	.	.	.	.	.	.	.	.	.	98.4
C3.6	.	.	.	.	.	.	.	.	.	.	.	.	.	1	14	.	.	.	.	.	.	.	.	.	.	.	.	.	.	.	.	.	.	.	.	.	.	.	.	.	93
D5.21	.	.	.	.	.	.	.	.	.	.	.	.	2	.	.	42	.	.	.	.	1	.	1	.	.	.	.	.	.	.	.	.	.	.	.	1	.	.	.	.	87.5
E1.91	.	.	.	.	.	.	.	.	.	.	.	.	.	.	.	.	113	.	.	.	.	.	.	.	.	.	.	.	.	.	.	.	.	.	.	.	.	.	.	.	100
E2.1	.	.	.	.	.	.	.	2	.	.	.	.	.	.	.	.	.	309	.	.	.	.	.	.	.	.	.	.	.	.	.	.	.	.	.	.	.	.	.	.	99.4
E2.1 X A5.1	.	.	.	.	.	.	.	.	.	.	.	.	.	.	.	.	.	.	81	.	.	.	.	.	.	.	.	.	.	.	.	.	.	.	.	.	.	.	.	.	100
E2.6	.	.	.	.	.	.	.	.	.	.	.	.	.	.	.	.	.	.	.	45	.	.	.	.	.	.	.	.	.	.	.	.	.	.	.	.	.	.	.	.	100
E3.41	.	.	.	.	.	.	.	2	.	.	.	.	.	.	.	.	.	1	.	.	703	.	.	.	.	.	.	.	.	.	.	.	.	.	.	.	.	.	.	.	99.6
E3.417	.	.	.	.	.	.	.	.	.	.	.	.	.	.	.	.	.	.	.	.	.	23	.	.	.	.	.	.	.	.	.	.	.	.	.	.	.	.	.	.	100.0
E3.44	.	.	.	.	.	.	.	.	.	.	.	.	.	.	.	.	.	.	.	.	.	.	246	.	.	.	.	.	.	.	.	.	.	.	.	.	.	.	.	.	100
E3.44 X A2.5	.	.	.	.	.	.	.	.	.	.	.	.	.	1	.	.	.	.	.	.	.	.	.	153	.	.	.	.	.	.	.	.	.	.	.	.	.	.	.	.	99.4
E3.441	.	.	.	.	.	.	.	.	.	.	.	.	.	.	.	.	.	.	.	.	.	.	.	.	101	.	.	.	.	.	.	.	.	.	.	.	.	.	.	.	100
E3.512	.	.	.	.	.	.	.	.	.	.	.	.	2	.	.	.	.	.	.	.	3	.	.	.	.	15	.	.	.	.	.	.	.	.	.	.	.	.	.	.	75.0
E5.1	.	.	.	.	.	.	.	1	.	.	.	.	.	.	.	.	.	.	.	.	.	.	.	2	.	.	30	.	.	.	.	.	.	.	.	.	.	.	.	.	90.9
E5.412	.	.	.	.	.	.	.	.	.	.	.	.	.	.	.	.	.	.	.	.	.	.	.	.	.	.	.	19	.	.	.	.	.	.	.	.	.	.	.	.	100
F3.111	.	.	.	.	.	.	.	.	.	.	.	.	.	.	.	.	1	.	.	.	.	.	1	.	.	.	.	.	89	.	.	.	.	.	.	.	.	.	.	.	97.8
F9.121	.	.	.	.	.	.	.	.	.	.	.	3	.	.	.	.	.	.	.	.	.	.	.	.	.	.	.	.	.	170	.	.	1	.	.	.	.	.	.	.	97.7
F9.2	.	.	.	.	.	.	.	.	.	.	.	.	.	.	.	.	.	.	.	.	2	.	.	.	.	.	.	.	.	.	61	.	2	.	.	3	.	.	.	.	89.7
F9.3131	.	.	.	.	.	.	.	.	.	.	.	.	.	.	.	.	.	.	.	.	.	.	.	.	.	.	.	.	.	.	.	34	.	.	.	.	.	.	.	.	100
G1.1111	.	.	.	.	.	.	.	.	.	.	.	2	.	.	.	.	.	.	.	.	.	.	.	.	.	.	.	.	.	4	1	.	124	.	1	2	.	.	.	.	92.5
G1.211	.	.	.	.	.	.	.	.	.	.	.	.	.	.	.	.	.	.	.	.	.	.	.	.	.	.	.	.	.	.	.	.	.	22	.	1	.	.	.	.	96
G1.22	.	.	.	.	.	.	.	.	.	.	.	.	.	.	.	.	.	.	.	.	.	.	.	.	.	.	.	.	.	1	.	.	4	.	83	1	.	.	.	.	93.3
G1.A1	.	.	.	.	.	.	.	.	.	.	.	.	.	.	.	.	.	.	.	.	.	.	.	.	1	.	.	.	2	.	.	.	.	.	.	265	1	.	.	.	98.5
G1.C1	.	.	.	.	.	.	.	.	.	.	.	.	.	.	.	.	.	.	.	.	.	.	.	.	.	.	.	.	.	.	.	.	.	.	.	.	136	.	.	.	100
G3.F12	.	.	.	.	.	.	.	.	.	.	.	.	.	.	.	.	.	.	.	.	.	.	.	.	.	.	.	.	.	.	.	.	.	.	.	.	.	113	.	.	100
I1.1	.	.	.	.	.	.	.	.	.	.	.	.	.	.	.	.	.	.	.	.	.	.	.	.	.	.	.	.	.	.	.	.	.	.	.	.	.	.	65	.	100
user's accuracy (%)	100	100	100	98.5	100	100	100	99.3	100	100	100	98.5	98.7	98.4	100	100	99.1	99.7	100	100	98.3	100	96.9	97.5	99.0	100	100	100	97.8	96.6	98.4	100	93.9	100	98.8	97.1	99.3	100	100	**OA : 98.7%** **Kappa: 0.99**

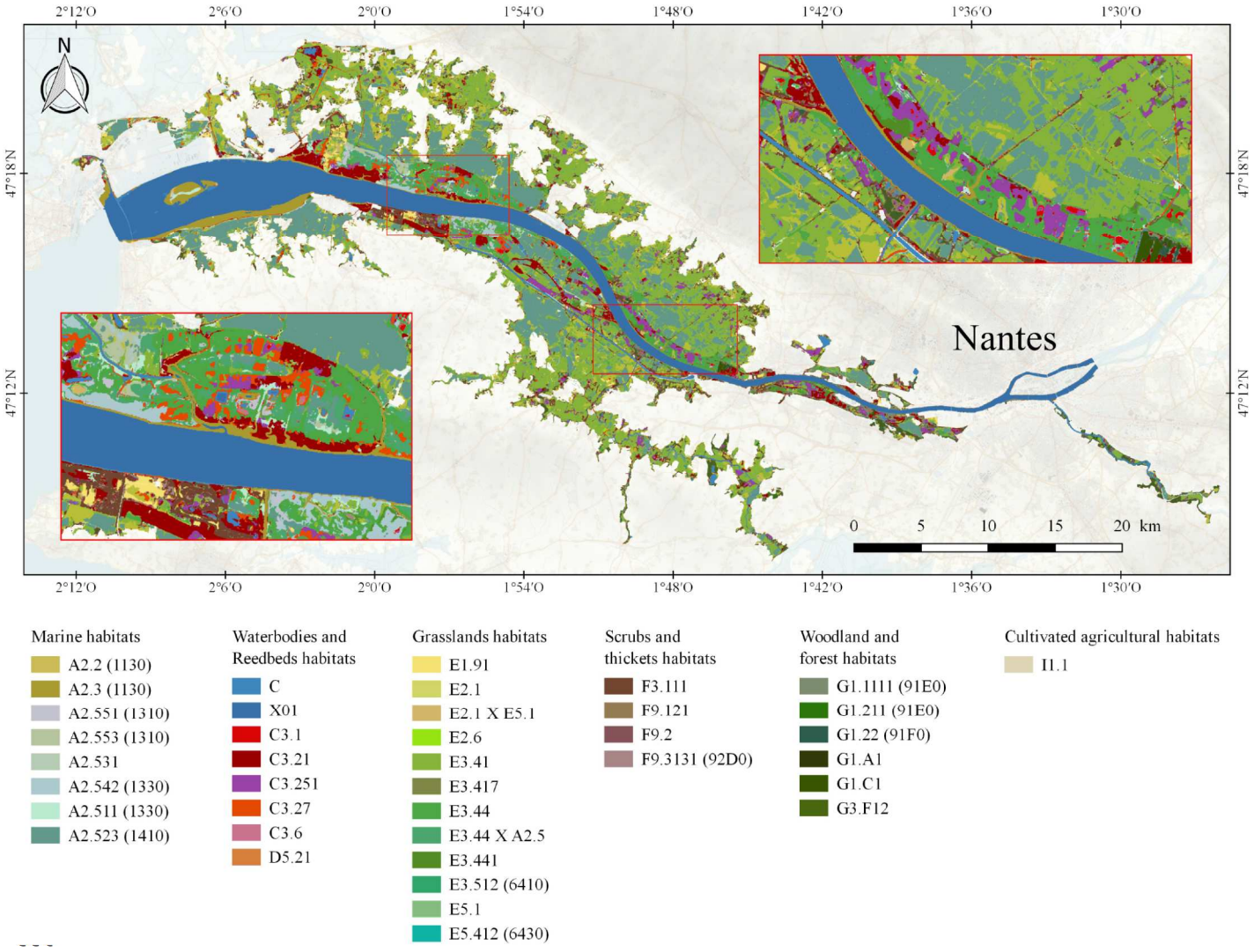

351 **Fig. 6.** Predicted map of the 39 EUNIS habitats in the Natura 2000 site 'Estuaire de la Loire'. The
352 codes correspond to EUNIS habitat identifiers and crosswalks with EUR28 habitats are indicated in
353 brackets. For details of the full habitat headings, see Table 3.

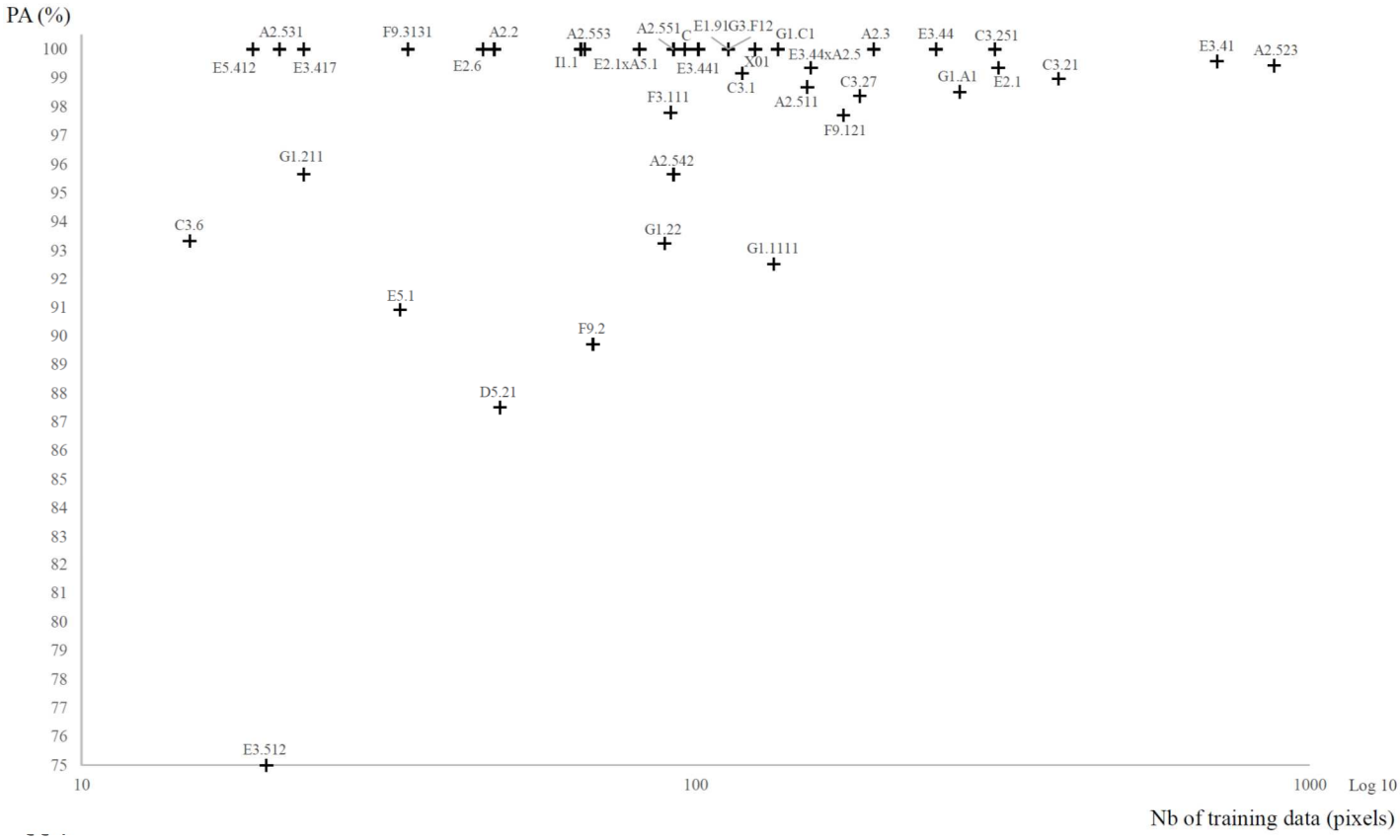

Fig. 7. Correspondence between the number of training data and the producers' accuracy (PA) for the 39 EUNIS habitats. Note that x-axis is in a log-scale.

3.5 Map description

Visually examining the final predictive map led us to evaluate qualitatively the consistency level with the reality in the field. Overall, the mapped units' distribution is consistent with the general organization of known habitats in the Loire estuary.

Marine habitats are distributed along both sides of the river downstream of the Natura 2000 site, which are most subject to oceanic influences. In these areas, Mediterranean salt meadows (EUNIS A2.523/EUR28 1410) cover vast areas homogeneously. Upstream, these salt meadows also develop in numerous areas as patches that mix with other habitats. Thus, these meadows represent the most extensive habitat with 5,047 ha mapped, corresponding to 19% of the study site's total surface.

Reed beds are frequently near the river, in areas that are regularly flooded by the tides. Among reed bed habitats, habitat C3.21 – '*Phragmites australis* beds' is dominating (977 ha) and regularly distributed in tidal marshes throughout the site. Habitat C3.27 – 'Halophile *Scirpus*, *Bolboschoenus* and *Schoenoplectus beds*' colonizes the downstream areas (510 ha) while habitat C3.251 – 'sweetgrass beds', intolerant to salt, succeeds it when going upstream (747 ha).

Grassland habitats also cover large areas (10,400 ha) and are distributed mostly upstream and on the margins of the site, i.e., in areas that are less subjected to saltwater intrusions. Thickets and forests are rarer and cover smaller areas with 1,471 ha and 1,027 ha respectively. These habitats usually do not tolerate salt, hence their location on the most upstream areas of the Natura 2000 site.

4. Discussion

4.1 The Importance of field data

Using a large amount of field data is paramount to ensure high accuracy in the classification of remotely sensed images (Calleja et al., 2019; Yeo et al., 2020). Several authors insist on using a wide range of vegetation plots to establish a complete typology of habitats (Chytrý et al., 2016; Rodwell et al., 2018). In this study, we relied on a large phytosociological plots dataset which led us to develop a complete and accurate typology of the study site. Beyond confirming the diversity of the habitats present at the Natura 2000 site, we used these field plots to calibrate the RF algorithm for image classification. Indeed, these field data are essential to locate and precisely sample the training areas to optimize image classification (Millard and Richardson, 2015). We conducted this step pixel by pixel by selecting only visually homogenous areas. The number of training pixels per habitat varies and depends on the number of field plots and habitat homogeneity. In general, the most widespread habitats are characterized by more training pixels to assess their variability at the scale of the study site (Colditz, 2015; Raab et al., 2018).

391 Most of the plots we used are derived from bibliographical data and were collected through an
392 important work of synthesis of the studies previously conducted on site (impact studies, vegetation
393 maps…). Accessing preexisting data is essential to develop a robust typology and to calibrate
394 classification algorithms. Thus, it is essential to centralize and share field plots, and especially to
395 implement common databases (Gautreau and Noucher, 2013), such as the European Vegetation
396 Archive which gathers thousands of vegetation plots across Europe (Chytrý et al., 2016).

397 However, despite compiling numerous phytosociological vegetation plots, we could only use a part to
398 calibrate the classifier. Indeed, several habitats could not be selected inside Sentinel-2 pixels because
399 the images' spatial resolution was insufficient to integrate habitats of small surface areas. This led us
400 to only use a partial typology of habitats compared to the initial typology established from all the
401 plots. For example, aquatic vegetation (i.e. *Lemnetalia minoris* or *Hydrocharition morsus-ranae*),
402 which are uncommon and occupy small areas, could not be represented in the final map. To overcome
403 this problem, other remote sensing images could be tested, such as high spatial resolution data (Gavish
404 et al., 2018; Strasser and Lang, 2015). For example, Espel et al. (2020) used very fine-scale resolution
405 Pléiades satellite imagery (50cm) to map aquatic vegetation in France.

406

407 *4.2 Single-date image classification*

408 *4.2.1 Determining the most favorable image acquisition dates*

409 Analysis of mono-temporal Sentinel-2 imagery showed that it is possible to obtain a satisfying level of
410 classification when using only one acquisition date. This is particularly the case for the image of July
411 6, 2019, for which we obtained an overall accuracy of 87.74%. Analysis of the overall accuracy (OA)
412 obtained for each date led us to determine the most favorable times of the year to get good
413 discrimination of the habitats. Even if the overall accuracy differences are small between dates
414 (Δ=11%), images acquired in spring and summer noticeably give the best results. This time of year is
415 especially marked by rapid phenological variations in vegetation (appearance of leaves, flowering).
416 Those variations are linked to the increase in day length and temperatures (Meier, 1997), as well as to

417 the receding water from winter flooding due in particular to evapotranspiration and the hydraulic
418 management of marshes (Reed, 1993). During this period of maximum vegetation growth, the plants'
419 expression of pigment content is most pronounced, favoring habitat discrimination (Addabbo et al.,
420 2016). These observations are consistent with the results of recent studies for vegetation mapping from
421 series of remote sensing images on floodplain meadows (Rapinel et al., 2019) or salt marsh vegetation
422 (Vrieling et al., 2018).

423

424 *4.2.2 Determination of the most favorable spectral bands and indices*

425 In this study, most habitats are characterized by vegetation whose spectral response is determined by
426 plants' biochemical and biophysical properties (Peñuelas and Filella, 1998). Over time, variations of
427 reflectance values and indices reflect plants' phytosociological changes (pigment composition, plants'
428 internal tissue structure) allow us to differentiate habitats according to their floristic composition (Cole
429 et al., 2014). MDG led us to highlight the most contributing variables for habitat mapping of the study
430 site.

431 B11 and B12 spectral bands appear as the best performing bands for all dates. These shortwave-
432 infrared (SWIR) spectral bands are especially characterized by their sensitivity to water on the earth's
433 surface (Middleton et al., 2012; Psomas et al., 2011) and to biochemical contents such as lignin and
434 cellulose in plant cover (Fourty et al., 1996). SWIR bands can be particularly useful for mapping
435 wetlands where plant communities are marked by flooding gradients (Rapinel et al., 2019). The B5
436 band is located at the beginning of the red-edge curve (704.1 nm), and it also represents an important
437 variable to discriminate the study site's habitats. Several studies have shown that different meadow
438 vegetation types can be effectively discriminated using red-edge wavelengths (Pinar and Curran, 1996;
439 Shoko and Mutanga, 2017) due to its sensitivity to variations in chlorophyll concentration (Curran et
440 al., 1990; Sims and Gamon, 2002). SWIR and red-edge spectrum regions are interesting for mapping
441 wetland vegetation as demonstrated by several previous studies (Dronova, 2015; Dronova et al., 2012;
442 Franke et al., 2012). GNDVI (based on NIR (B8) and green (B3) bands) is the most important

vegetation index in this study. It is a variation of NDVI but is found to be more sensitive to plants' changes in chlorophyll content (Gitelson et al., 1996). For instance, GNDVI provided a good distinction between vegetated and non-vegetated habitats characterized by high and low values of the index respectively.

The other retained variables contribute to a lesser extent: MTCI (analysis of the red-edge curve with B4, B6 and B5), B3 (leaf green intensity), NDWI (leaf water content with B8 and B11), B2 (leaf blue-green intensity), EVI (leaf pigment content with B2, B4 and B8) and B8A (leaf structure). Overall, we notice that most available spectral bands contributed to the classifications' success. Thus, our results confirm the relevance of the different spectral regions covered by Sentinel-2 satellites for vegetation mapping (Fauvel et al., 2020; Grabska et al., 2019).

4.3 Multi-date classification

While individual image analyses achieved satisfactory levels of accuracy, the multi-date classification considerably improved habitats modeling accuracy with a 98.8% OA and a 0.99 Kappa. PA and UA are at 100% for numerous habitats showing a perfect match between reference and modeled data. For the other habitats, PA and UA are still very close to 100%, thus indicating respectively low over-or under-representation in the final map.

Numerous authors demonstrated the accuracy improvement brought by multi-date classifications compared to single-date classifications (Belgiu and Csillik, 2018; Feret et al., 2015; Raab et al., 2018). Rapinel et al. (2019) especially highlighted the benefits of a Sentinel-2 multi-date classification to differentiate marsh plant communities according to the flood duration and management measures (mowing, grazing). In the same way, the evolution of these parameters during our study period contributed to the success of the habitat classification of the Loire estuary.

4.4 Habitat mapping by remote sensing: contributions for nature conservation

Our work led us to elaborate a map of EUNIS habitats from which it is possible to highlight conservation issues, specifically those linked to the European Habitat Directive (HabDir). Even if we could not map all the habitats of community interests due to their small surface areas, we mapped 9 HCIs from typological crosswalks, representing a total of 7,080 ha, i.e. 26% of the total surface area of the site. Among all the habitats, HCI 1410 'Mediterranean salt meadows (*Juncetalia maritimi*)' covers the largest area (5,047 ha, 19% of the total surface area). Thus, the use of Sentinel-2 images contributes to locate and quantify the occupied areas for these habitats of the Natura 2000 site: distribution and range being two parameters retained to assess the conservation status according to Art.17 of HabDir (European Commission, 1992; DG Environment, 2017). These data are essential for managers to define conservation measures to maintain the HICs. Thus, the habitat map produced during this study meets the needs of the manager of the Natura 2000 site 'Estuaire de la Loire' and will be essential to preserve this natural site.

Overall, our results show that it is possible to obtain habitat maps quickly and at a low cost compared with conventional fieldwork (Ichter et al., 2014). This method can be transposed to other natural sites, in or outside the Natura 2000 network, which has the advantage of promoting a common and standardized methodological approach to habitat mapping. In addition, the approach we offer completely meets the European requirements as part of the reporting required by Europe for each member state. Indeed, this method could be adopted to evaluate the distribution and areas of habitats at the European scale, two parameters defined by the HabDir to assess the conservation status of HICs (Bijlsma et al., 2019; Gigante et al., 2016). Furthermore, this method can be used for long-term monitoring of habitats based on regularly produced maps (every three or four years depending on the habitat type). The approach we developed meets the need for a monitoring method which could be proposed as part of Art. 11 of HabDir on surveillance of the conservation status of HICs (Delbosc et al. 2021).

5. Conclusion

Our results demonstrated that Sentinel-2 images allow for accurately mapping habitats and that their spectral resolution is particularly adapted to the study of wetlands. The high revisit frequency of Sentinel-2 satellites ensures the regular acquisition of images throughout the year, allowing multi-date image classification. This method led us to obtain a highly accurate habitat map, which considerably improves the accuracy level compared to single-date image classification. However, the spatial resolution of Sentinel-2 remains insufficient to include numerous habitats that are only locally and occasionally present. In this study, only 23 out of the 62 EUNIS habitats could be mapped. Consequently, using these images can only be considered to map habitats with a surface area higher than 100 m². Our results generally show that Sentinel-2 data are adapted to create habitat maps at a 1:25 000 scale. For finer-scale mapping, Sentinel-2 could be complemented by high spatial resolution remote sensing data such as those provided by other satellites, UAV or airborne acquisitions.

Funding

This research was carried out as part of a PhD CIFRE studentship funding co-financed by ANRT (national research-technology association), the European Regional Development Fund (ERDF) and the Ministry of Ecology within the framework of the financial agreement for the animation of the Natura 2000 site 'Estuaire de la Loire'.

Acknowledgments

The authors would like to thank Kristell Le Bot (GIP Loire-Estuaire), Bérengère Autret (Grand Port Maritime Nantes Saint-Nazaire) and Aline Corbeaux (Nantes Métropole) for providing vegetation-plot data for this study. We would like to thank all the people involved in collecting field data. The authors would particularly like to thank Hermann Guitton of the National Botanical Conservatory of Brest for his assistance in field investigations, bibliographic data collection and useful discussions. Stéphanie Trécant and Frédéric Moré are gratefully acknowledged for their assistance in financially setting up

519 this project. We also wish to thank Cassandra Carnet for her contribution to translating the work into
520 English. We are grateful to the two anonymous reviewers for providing constructive comments on the
521 manuscript, improving the overall quality of the paper.

522

523 **References**

524 Adam, E., Mutanga, O., Rugege, D., 2010. Multispectral and hyperspectral remote sensing for identification and
525 mapping of wetland vegetation: A review. Wetl. Ecol. Manag. 18, 281–296.
526 https://doi.org/10.1007/s11273-009-9169-z

527 Addabbo, P., Focareta, M., Marcuccio, S., Votto, C., Ullo, S.L., 2016. Contribution of Sentinel-2 data for
528 applications in vegetation monitoring. Acta IMEKO. https://doi.org/10.21014/acta_imeko.v5i2.352

529 Belgiu, M., Csillik, O., 2018. Sentinel-2 cropland mapping using pixel-based and object-based time-weighted
530 dynamic time warping analysis. Remote Sens. Environ. 204, 509–523.
531 https://doi.org/10.1016/j.rse.2017.10.005

532 Bensettiti F., Rameau J.-C. & Chevallier H. (coord.), 2001. « Cahiers d'habitats » Natura 2000. Connaissance et
533 gestion des habitats et des espèces d'intérêt communautaire. Tome 1 - Habitats forestiers. MATE / MAP /
534 MNHN. Éd. La Documentation francaise, Paris, 2 volumes : 339 p. et 423 p. + cédérom.

535 Bensettiti F., Bioret F., Roland J. & Lacoste J.-P. (coord.), 2004. « Cahiers d'habitats » Natura 2000.
536 Connaissance et gestion des habitats et des espèces d'intérêt communautaire. Tome 2 - Habitats côtiers.
537 MEDD / MAAPAR / MNHN. Éd. La Documentation francaise, Paris, 399 p. + cédérom.

538 Bensettiti F., Gaudillat V. & Haury J. (coord.), 2002. « Cahiers d'habitats » Natura 2000. Connaissance et
539 gestion des habitats et des espèces d'intérêt communautaire. Tome 3 - Habitats humides. MATE / MAP /
540 MNHN. Éd. La Documentation francaise, Paris, 457 p. + cédérom.

541 Bensettiti F., Boullet V., Chavaudret-Laborie C. & Deniaud J. (coord.), 2005. « Cahiers d'habitats » Natura 2000.
542 Connaissance et gestion des habitats et des espèces d'intérêt communautaire. Tome 4 - Habitats
543 agropastoraux. MEDD / MAAPAR / MNHN. Éd. La Documentation francaise, Paris, 2 volumes : 445 p. et
544 487 p. + cédérom.

545 Bijlsma, R.J., Agrillo, E., Attorre, F., Boitani, L., Brunner, A., Evans, P., Foppen, R., Gubbay, S., Janssen,
546 J.A.M., van Kleunen, A., Langhout, W., Pacifici, M., Ramirez, I., Rondinini, C., van Roomen, M., Siepel,
547 H., van Swaaij, C.A.M., Winter, H.V., 2019. Defining and applying the concept of Favourable Reference
548 Values for species habitats under the EU Birds and Habitats Directives : examples of setting favourable
549 reference values. https://doi.org/10.18174/468534

550 Bioret, F., Gaudillat, V., Royer, J.-M., 2013. The Prodrome of French vegetation: a national synsystem for
551 phytosociological knowledge and management issues. Plant Sociol. 50, 17–21.

552 Bivand, R., Keitt, T. & Rowlingson, B. 2015. Rgdal: Bindings for the Geospatial Data Abstraction Library.
553 Retrieved from http://CRAN.R-project.org/package=rgdal

554 Blackburn, G.A., 1998. Quantifying Chlorophylls and Caroteniods at Leaf and Canopy Scales. Remote Sens.
555 Environ. 66, 273–285. https://doi.org/10.1016/S0034-4257(98)00059-5

556 Braun-Blanquet, J., 1932. Plant Sociology the Study of Plant Communities. McGraw- Hill Book Company, New
557 York, London.

558 Breiman, L., 2001. Random forests. Machine Learning, 45(1), 5–32.

559 Bunce, R.G.H., Bogers, M.M.B., Evans, D., Halada, L., Jongman, R.H.G., Mucher, C.A., Bauch, B., De Blust,
560 G., Parr, T.W., Olsvig-Whittaker, L., 2013. The significance of habitats as indicators of biodiversity and
561 their links to species. Ecol. Indic. 33, 19–25. https://doi.org/10.1016/j.ecolind.2012.07.014

562 Calleja, F., Ondiviela, B., Galván, C., Recio, M., Juanes, J.A., 2019. Mapping Estuarine Vegetation Using
563 Satellite Imagery: The case of the invasive species Baccharis halimifolia at a Natura 2000 site. Cont. Shelf
564 Res. https://doi.org/10.1016/j.csr.2019.01.002

565 Cherrill, A., 2014. The occurrence , causes and consequences of inter-observer variation in identification of
566 vegetation types and recommendations for improvements to standard ecological survey methods. Harper
567 Adams Univ.

568 Chytrý, M., Hennekens, S.M., Jiménez-Alfaro, B., Knollová, I., Dengler, J., Jansen, F., Landucci, F., Schaminée,
569 J.H.J., Aćić, S., Agrillo, E., Ambarlı, D., Angelini, P., Apostolova, I., Attorre, F., Berg, C., Bergmeier, E.,
570 Biurrun, I., Botta-Dukát, Z., Brisse, H., Campos, J.A., Carlón, L., Čarni, A., Casella, L., Csiky, J.,
571 Ćušterevska, R., Dajić Stevanović, Z., Danihelka, J., De Bie, E., de Ruffray, P., De Sanctis, M., Dickoré,

572 W.B., Dimopoulos, P., Dubyna, D., Dziuba, T., Ejrnaes, R., Ermakov, N., Ewald, J., Fanelli, G.,
573 Fernández-González, F., FitzPatrick, Ú., Font, X., García-Mijangos, I., Gavilán, R.G., Golub, V., Guarino,
574 R., Haveman, R., Indreica, A., Işık Gürsoy, D., Jandt, U., Janssen, J.A.M., Jiroušek, M., Kącki, Z.,
575 Kavgacı, A., Kleikamp, M., Kolomiychuk, V., Krstivojević Ćuk, M., Krstonošić, D., Kuzemko, A., Lenoir,
576 J., Lysenko, T., Marcenò, C., Martynenko, V., Michalcová, D., Moeslund, J.E., Onyshchenko, V.,
577 Pedashenko, H., Pérez-Haase, A., Peterka, T., Prokhorov, V., Rašomavičius, V., Rodríguez-Rojo, M.P.,
578 Rodwell, J.S., Rogova, T., Ruprecht, E., Rūsiņa, S., Seidler, G., Šibík, J., Šilc, U., Škvorc, Ž., Sopotlieva,
579 D., Stančić, Z., Svenning, J.-C., Swacha, G., Tsiripidis, I., Turtureanu, P.D., Uğurlu, E., Uogintas, D.,
580 Valachovič, M., Vashenyak, Y., Vassilev, K., Venanzoni, R., Virtanen, R., Weekes, L., Willner, W.,
581 Wohlgemuth, T., Yamalov, S., 2016. European Vegetation Archive (EVA): an integrated database of
582 European vegetation plots. Appl. Veg. Sci. 19, 173–180. https://doi.org/10.1111/avsc.12191

583 Chytrý, M., Tichý, L., Hennekens, S.M., Knollová, I., Janssen, J.A.M., Rodwell, J.S., Peterka, T., Marcenò, C.,
584 Landucci, F., Danihelka, J., Hájek, M., Dengler, J., Novák, P., Zukal, D., Jiménez-Alfaro, B., Mucina, L.,
585 Abdulhak, S., Aćić, S., Agrillo, E., Attorre, F., Bergmeier, E., Biurrun, I., Boch, S., Bölöni, J., Bonari, G.,
586 Braslavskaya, T., Bruelheide, H., Campos, J.A., Čarni, A., Casella, L., Ćuk, M., Ćušterevska, R., De Bie,
587 E., Delbosc, P., Demina, O., Didukh, Y., Dítě, D., Dziuba, T., Ewald, J., Gavilán, R.G., Gégout, J., Giusso
588 del Galdo, G. Pietro, Golub, V., Goncharova, N., Goral, F., Graf, U., Indreica, A., Isermann, M., Jandt, U.,
589 Jansen, F., Jansen, J., Jašková, A., Jiroušek, M., Kącki, Z., Kalníková, V., Kavgacı, A., Khanina, L., Yu.
590 Korolyuk, A., Kozhevnikova, M., Kuzemko, A., Küzmič, F., Kuznetsov, O.L., Laiviņš, M., Lavrinenko, I.,
591 Lavrinenko, O., Lebedeva, M., Lososová, Z., Lysenko, T., Maciejewski, L., Mardari, C., Marinšek, A.,
592 Napreenko, M.G., Onyshchenko, V., Pérez-Haase, A., Pielech, R., Prokhorov, V., Rašomavičius, V.,
593 Rodríguez Rojo, M.P., Rūsiņa, S., Schrautzer, J., Šibík, J., Šilc, U., Škvorc, Ž., Smagin, V.A., Stančić, Z.,
594 Stanisci, A., Tikhonova, E., Tonteri, T., Uogintas, D., Valachovič, M., Vassilev, K., Vynokurov, D.,
595 Willner, W., Yamalov, S., Evans, D., Palitzsch Lund, M., Spyropoulou, R., Tryfon, E., Schaminée, J.H.J.,
596 2020. EUNIS Habitat Classification: Expert system, characteristic species combinations and distribution
597 maps of European habitats. Appl. Veg. Sci. avsc.12519. https://doi.org/10.1111/avsc.12519

598 Clair, M., Gaudillat, V., Michez, N., & Poncet R., 2019. HABREF v5.0, référentiel des typologies d'habitats et
599 de végétation pour la France. Guide méthodologique. Rapport UMS PatriNat (AFB-CNRS-MNHN), Paris,
600 95 p.

601 Colditz, R.R., 2015. An evaluation of different training sample allocation schemes for discrete and continuous

land cover classification using decision tree-based algorithms. Remote Sens. 7, 9655–9681. https://doi.org/10.3390/rs70809655

Congalton, R.G., 1991. A review of assessing the accuracy of classifications of remotely sensed data. Remote Sens. Environ. 37, 35–46. https://doi.org/10.1016/0034-4257(91)90048-B

Corbane, C., Lang, S., Pipkins, K., Alleaume, S., Deshayes, M., Garc??a Mill??n, V.E., Strasser, T., Vanden Borre, J., Toon, S., Michael, F., 2015. Remote sensing for mapping natural habitats and their conservation status - New opportunities and challenges. Int. J. Appl. Earth Obs. Geoinf. 37, 7–16. https://doi.org/10.1016/j.jag.2014.11.005

Curran, P.J., Dungan, J.L., Gholz, H.L., 1990. Exploring the relationship between reflectance red edge and chlorophyll content in slash pine. Tree Physiol. 7, 33–48. https://doi.org/10.1093/treephys/7.1-2-3-4.33

Dronova, I., 2015. Object-based image analysis in wetland research: A review. Remote Sens. 7, 6380–6413. https://doi.org/10.3390/rs70506380

Dronova, I., Gong, P., Clinton, N.E., Wang, L., Fu, W., Qi, S., Liu, Y., 2012. Landscape analysis of wetland plant functional types:. 127, 357–369. https://doi.org/10.1016/j.rse.2012.09.018

Dash, J., Curran, P.J., 2004. The MERIS terrestrial chlorophyll index. Int. J. Remote Sens. 25, 5403–5413. https://doi.org/10.1080/0143116042000274015

Daughtry, C., 2000. Estimating Corn Leaf Chlorophyll Concentration from Leaf and Canopy Reflectance. Remote Sens. Environ. 74, 229–239. https://doi.org/10.1016/S0034-4257(00)00113-9

Dengler, J., Chytrý, M.,Ewald, J., 2008. Phytosociology, in: Jørgensen S.E., Fath B.D. (eds.), General Ecology. Vol. 4 of Encyclopedia of Ecology, Elsevier, Oxford, pp. 2767–2779.

Delbosc P., Lagrange I., Rozo C., Bensettiti F., Bouzillé J.-B., Evans D., Lalanne A., Rapinel S., Bioret F., 2021). Assessing the conservation status of coastal habitats under Article 17 of the EU Habitats Directive. Biological Conservation, 254 (October 2020). https://doi.org/10.1016/j.biocon.2020.108935

Delegido, J., Verrelst, J., Alonso, L., Moreno, J., 2011. Evaluation of Sentinel-2 Red-Edge Bands for Empirical Estimation of Green LAI and Chlorophyll Content. Sensors 11, 7063–7081. https://doi.org/10.3390/s110707063

DG Environment, 2017. Reporting under Article 17 of the Habitats Directive: Explanatory notes and guidelines

for the period 2013–2018. Final version – May 2017. Brussels, 1 –188. http://cdr.eionet.europa.eu/help/habitats_art17/index_htm

European Commission, 1992. Council Directive 92/43/EEC of 21 May 1992 on the conservation of natural habitats and of wild fauna and flora. Official Journal of the European Union 1992, 206, 7–50

European Commission, 2013. Interpretation manual of European union habitats—EUR28. Bruxelles, Belgium: European Commission DG Environment Nature

Evans, D., 2012. Building the European Union's Natura 2000 network. Nat. Conserv. 1, 11–26. https://doi.org/10.3897/natureconservation.1.1808

Evans, D., Arvela, M., 2011. Assessment and reporting under Article 17 of the Habitats Directive. Explanatory Notes & Guidelines for the period 2007-2012. European Commission, Brussels, pp. 123.

Fauvel, M., Lopes, M., Dubo, T., Rivers-Moore, J., Frison, P.-L., Gross, N., Ouin, A., 2020. Prediction of plant diversity in grasslands using Sentinel-1 and -2 satellite image time series. Remote Sens. Environ. 237, 111536. https://doi.org/10.1016/J.RSE.2019.111536

Feret, J.B., Corbane, C., Alleaume, S., 2015. Detecting the Phenology and Discriminating Mediterranean Natural Habitats with Multispectral Sensors-An Analysis Based on Multiseasonal Field Spectra. IEEE J. Sel. Top. Appl. Earth Obs. Remote Sens. 8, 2294–2305. https://doi.org/10.1109/JSTARS.2015.2431320

Fourty, T., Baret, F., Jacquemoud, S., Schmuck, G., Verdebout, J., 1996. Leaf optical properties with explicit description of its biochemical composition: Direct and inverse problems. Remote Sens. Environ. 56, 104–117. https://doi.org/10.1016/0034-4257(95)00234-0

Franke, J., Navratil, P., Keuck, V., Peterson, K., Siegert, F., 2012. Monitoring Fire and Selective Logging Activities in Tropical Peat Swamp Forests. IEEE J. Sel. Top. Appl. Earth Obs. Remote Sens. 5, 1811–1820. https://doi.org/10.1109/JSTARS.2012.2202638

Gautreau, P., Noucher, M., 2013. Gouvernance informationnelle de l'environnement et partage en ligne des données publiques. Netcom, 27-1/2, 5-21.

Gao, B., 1996. NDWI—A normalized difference water index for remote sensing of vegetation liquid water from space. Remote Sens. Environ. 58, 257–266. https://doi.org/10.1016/S0034-4257(96)00067-3

Gavish, Y., O'Connell, J., Marsh, C.J., Tarantino, C., Blonda, P., Tomaselli, V., Kunin, W.E., 2018. Comparing

656 the performance of flat and hierarchical Habitat/Land-Cover classification models in a NATURA 2000
657 site. ISPRS J. Photogramm. Remote Sens. 136, 1–12. https://doi.org/10.1016/j.isprsjprs.2017.12.002

658 Gayet, G., Baptist, F., Maciejewski, L., Poncet, R., Bensettiti, F., 2018. Guide de détermination des habitats
659 terrestres et marins de la typologie EUNIS - version 1.0. AFB, collection Guides et protocoles, 230 pages

660 Gigante, D., Foggi, B., Venanzoni, R., Viciani, D., Buffa, G., 2016. Habitats on the grid: The spatial dimension
661 does matter for red-listing. J. Nat. Conserv. 32, 1–9. https://doi.org/10.1016/j.jnc.2016.03.007

662 Gitelson, A.A., Kaufman, Y.J., Merzlyak, M.N., 1996. Use of a green channel in remote sensing of global
663 vegetation from EOS-MODIS. Remote Sens. Environ. 58, 289–298. https://doi.org/10.1016/S0034-
664 4257(96)00072-7

665 Gitelson, A.A., Viña, A., Verma, S.B., Rundquist, D.C., Arkebauer, T.J., Keydan, G., Leavitt, B., Ciganda, V.,
666 Burba, G.G., Suyker, A.E., 2006. Relationship between gross primary production and chlorophyll content
667 in crops: Implications for the synoptic monitoring of vegetation productivity. J. Geophys. Res. 111,
668 D08S11. https://doi.org/10.1029/2005JD006017

669 Grabska, E., Hostert, P., Pflugmacher, D., Ostapowicz, K., 2019. Forest stand species mapping using the
670 sentinel-2 time series. Remote Sens. 11, 1–24. https://doi.org/10.3390/rs11101197

671 Haest, B., Borre, J. Vanden, Spanhove, T., Thoonen, G., Delalieux, S., Kooistra, L., Mücher, C.A., Paelinckx,
672 D., Scheunders, P., Kempeneers, P., 2017. Habitat mapping and quality assessment of NATURA 2000
673 heathland using airborne imaging spectroscopy. Remote Sens. 9. https://doi.org/10.3390/rs9030266

674 Harris, A., Charnock, R., Lucas, R.M., 2015. Hyperspectral remote sensing of peatland floristic gradients.
675 Remote Sens. Environ. 162, 99–111. https://doi.org/10.1016/j.rse.2015.01.029

676 Hijmans, R.J. 2015. Raster: Geographic Data Analysis and Modeling. Retrieved from http://CRAN.R-
677 project.org/ package=raster

678 Huete, A.., 1988. A soil-adjusted vegetation index (SAVI). Remote Sens. Environ. 25, 295–309.
679 https://doi.org/10.1016/0034-4257(88)90106-X

680 Huete, A., Didan, K., Miura, T., Rodriguez, E.., Gao, X., Ferreira, L.., 2002. Overview of the radiometric and
681 biophysical performance of the MODIS vegetation indices. Remote Sens. Environ. 83, 195–213.
682 https://doi.org/10.1016/S0034-4257(02)00096-2

683 Ichter, J., Evans, D., Dominique, R., 2014. Terrestrial habitat mapping in Europe: an overview.
684 https://doi.org/10.2800/11055

685 Inglada, J., Vincent, A., Arias, M., Tardy, B., Morin, D., Rodes, I., 2017. Operational High Resolution Land
686 Cover Map Production at the Country Scale Using Satellite Image Time Series. Remote Sens. 9, 95.
687 https://doi.org/10.3390/rs9010095

688 Kaplan, G., Avdan, U., 2017. Mapping and Monitoring Wetlands Using SENTINEL-2 Satellite Imagery. ISPRS
689 Ann. Photogramm. Remote Sens. Spat. Inf. Sci. IV, 271–277.

690 Kopeć, D., Michalska-Hejduk, D., Sławik, Ł., Berezowski, T., Borowski, M., Rosadziński, S., Chormański, J.,
691 2016. Application of multisensoral remote sensing data in the mapping of alkaline fens Natura 2000
692 habitat. Ecol. Indic. 70, 196–208. https://doi.org/10.1016/j.ecolind.2016.06.001

693 Kuhn, M., 2012. Variable Selection Using the Caret Package. (URL Httpcran Cermin Lipi Go
694 IdwebpackagescaretvignettescaretSelection Pdf).

695 Lang, S., Mairota, P., Pernkopf, L., Schioppa, E.P., 2015. Earth observation for habitat mapping and biodiversity
696 monitoring. Int. J. Appl. Earth Obs. Geoinf. 37, 1–6. https://doi.org/10.1016/j.jag.2014.10.007

697 Meier, U. (ed.): Growth stages of Mono- and Dicotyledonus Plants. BBCH Monograph, Blackwell
698 Wissenschafts-Verlag Berlin Wien, 622pp, 1997

699 Le Dez, M., Sawtschuk, J., Bioret, F., 2017. Les prairies de l'estuaire de la Loire : étude de la dynamique de la
700 végétation de 1982 à 2014. Mappemonde 119, 1–18. https://doi.org/10.4000/mappemonde.2097

701 Liaw, A. and Wiener, M. (2002) Classification and Regression by Random Forest. R News, 2, 18-22.

702 Marzialetti, F., Giulio, S., Malavasi, M., Sperandii, M.G., Acosta, A.T.R., Carranza, M.L., 2019. Capturing
703 coastal dune natural vegetation types using a phenology-based mapping approach: The potential of
704 Sentinel-2. Remote Sens. 11. https://doi.org/10.3390/rs11121506

705 Middleton, M., Närhi, P., Arkimaa, H., Hyvönen, E., Kuosmanen, V., Treitz, P., Sutinen, R., 2012. Ordination
706 and hyperspectral remote sensing approach to classify peatland biotopes along soil moisture and fertility
707 gradients. Remote Sens. Environ. 124, 596–609. https://doi.org/10.1016/j.rse.2012.06.010

708 Millard, K., Richardson, M., 2015. On the importance of training data sample selection in Random Forest image
709 classification: A case study in peatland ecosystem mapping. Remote Sens. 7, 8489–8515.

https://doi.org/10.3390/rs70708489

Moran, N., Nieland, C. machine learning and ontological data handling for multi-source classification of nature conservation areas S., Tintrup gen. Suntrup, G., Kleinschmit, B., 2017. Combining machine learning and ontological data handling for multi-source classification of nature conservation areas. Int. J. Appl. Earth Obs. Geoinf. 54, 124–133. https://doi.org/10.1016/j.jag.2016.09.009

Peñuelas, J., Filella, I., 1998. Visible and near-infrared reflectance techniques for diagnosing plant physiological status. Trends Plant Sci. 3, 151–156. https://doi.org/10.1016/S1360-1385(98)01213-8

Pinar, A., Curran, P.J., 1996. Technical Note Grass chlorophyll and the reflectance red edge. Int. J. Remote Sens. 17, 351–357. https://doi.org/10.1080/01431169608949010

Psomas, A., Kneubühler, M., Huber, S., Itten, K., Zimmermann, N.E., 2011. Hyperspectral remote sensing for estimating aboveground biomass and for exploring species richness patterns of grassland habitats. Int. J. Remote Sens. 32, 9007–9031. https://doi.org/10.1080/01431161.2010.532172

QGIS Development Team, 2019. QGIS Geographic Information System (Version 3.4.8). Open Source Geospatial Foundation. URL http://qgis.org

R Development Core Team (2019). R: A Language and Environment for Statistical Computing. Vienna, Austria: R Foundation for Statistical Computing.

Raab, C., Stroh, H.G., Tonn, B., Meißner, M., Rohwer, N., Balkenhol, N., Isselstein, J., Raab, C., Stroh, H.G., Tonn, B., Meißner, M., Rohwer, N., Balkenhol, N., 2018. Mapping semi-natural grassland communities using multi-temporal RapidEye remote sensing data. Int. J. Remote Sens. 00, 1–22. https://doi.org/10.1080/01431161.2018.1504344

Radecka, A., Michalska-Hejduk, D., Osińska-Skotak, K., Kania, A., Górski, K., Ostrowski, W., 2019. Mapping secondary succession species in agricultural landscape with the use of hyperspectral and airborne laser scanning data. J. Appl. Remote Sens. 13, 1. https://doi.org/10.1117/1.jrs.13.034502

Rapinel, S., Clément, B., Magnanon, S., Sellin, V., Hubert-Moy, L., 2014. Identification and mapping of natural vegetation on a coastal site using a Worldview-2 satellite image. J. Environ. Manage. 144, 236–246. https://doi.org/10.1016/j.jenvman.2014.05.027

Rapinel, S., Hubert-Moy, L., Clément, B., 2015. Combined use of lidar data and multispectral earth observation

737 imagery for wetland habitat mapping. Int. J. Appl. Earth Obs. Geoinf. 37, 56–64.
738 https://doi.org/10.1016/j.jag.2014.09.002

739 Rapinel, S., Mony, C., Lecoq, L., Clément, B., Thomas, A., Hubert-moy, L., 2019. Evaluation of Sentinel-2
740 time-series for mapping fl oodplain grassland plant communities. Remote Sens. Environ. 223, 115–129.
741 https://doi.org/10.1016/j.rse.2019.01.018

742 Rapinel, S., Rozo, C., Delbosc, P., Bioret, F., Bouzillé, J., Hubert-Moy, L., 2020. Contribution of free satellite
743 time-series images to mapping plant communities in the Mediterranean Natura 2000 site: the example of
744 Biguglia Pond in Corse (France). Mediterr. Bot. 41, 181–191. https://doi.org/10.5209/mbot.66535

745 Reed, D.J., 1993. Hydrology of temperate wetlands. Prog. Phys. Geogr. Earth Environ. 17, 20–31.
746 https://doi.org/10.1177/030913339301700102

747 Roberts, D., Roth, K., Perroy, R., 2011. Hyperspectral Vegetation Indices, in: Hyperspectral Remote Sensing of
748 Vegetation. CRC Press, pp. 309–328. https://doi.org/10.1201/b11222-20

749 Rodwell, J.S., Evans, D., Schaminée, J.H.J., 2018. Phytosociological relationships in European Union policy-
750 related habitat classifications. Rend. Lincei 29, 237–249. https://doi.org/10.1007/s12210-018-0690-y

751 Rouse, J.W., Haas, R.H., Schell, J.A., Deering, W.D., 1973. Monitoring vegetation systems in the Great Plains
752 with ERTS. In: Third ERTS Symposium, NASA SP-351, pp. 309–317.

753 Schaminée, J.H.J., Chytry, M., Dengler, J., Hennekens, S., Janssen, J.A.M., Jiménez-Alfaro, B., Knollova, I.,
754 Landucci, F., Marcenò, C., Rodwell, J.S., Tichi, L., 2016. Development of distribution maps of grassland
755 habitats of EUNIS habitat classification. https://doi.org/10.13140/RG.2.2.31608.44802

756 Schuster, C., Schmidt, T., Conrad, C., Kleinschmit, B., F??rster, M., 2015. Grassland habitat mapping by intra-
757 annual time series analysis -Comparison of RapidEye and TerraSAR-X satellite data. Int. J. Appl. Earth
758 Obs. Geoinf. 34, 25–34. https://doi.org/10.1016/j.jag.2014.06.004

759 Shoko, C., Mutanga, O., 2017. Examining the strength of the newly-launched Sentinel 2 MSI sensor in detecting
760 and discriminating subtle differences between C3 and C4 grass species. ISPRS J. Photogramm. Remote
761 Sens. 129, 32–40. https://doi.org/10.1016/j.isprsjprs.2017.04.016

762 Sims, D.A., Gamon, J.A., 2002. Relationships between leaf pigment content and spectral reflectance across a
763 wide range of species, leaf structures and developmental stages. Remote Sens. Environ. 81, 337–354.

https://doi.org/10.1016/S0034-4257(02)00010-X

Sławik, Ł., Niedzielko, J., Kania, A., Piórkowski, H., Kopeć, D., 2019. Multiple flights or single flight instrument fusion of hyperspectral and ALS data? A comparison of their performance for vegetation mapping. Remote Sens. 11. https://doi.org/10.3390/rs11080913

Smits, P.C., Dellepiane, S.G., Schowengerdt, R.A., 1999. Quality assessment of image classification algorithms for land-cover mapping: A review and a proposal for a cost-based approach. Int. J. Remote Sens. 20, 1461–1486. https://doi.org/10.1080/014311699212560

Stehman, S. V., 1997. Selecting and interpreting measures of thematic classification accuracy. Remote Sens. Environ. 62, 77–89. https://doi.org/10.1016/S0034-4257(97)00083-7

Stenzel, S., Feilhauer, H., Mack, B., Metz, A., Schmidtlein, S., 2014. Remote sensing of scattered natura 2000 habitats using a one-class classifier. Int. J. Appl. Earth Obs. Geoinf. 33, 211–217. https://doi.org/10.1016/j.jag.2014.05.012

Strasser, T., Lang, S., 2015. Object-based class modelling for multi-scale riparian forest habitat mapping. Int. J. Appl. Earth Obs. Geoinf. 37, 29–37. https://doi.org/10.1016/j.jag.2014.10.002

Tigges, J., Lakes, T., Hostert, P., 2013. Urban vegetation classification: Benefits of multitemporal RapidEye satellite data. Remote Sens. Environ. 136, 66–75. https://doi.org/10.1016/j.rse.2013.05.001

Ullerud, H.A., Bryn, A., Halvorsen, R., Hemsing, L.Ø., 2018. Consistency in land-cover mapping: Influence of field workers, spatial scale and classification system. Appl. Veg. Sci. 21, 278–288. https://doi.org/10.1111/avsc.12368

Vanden Borre, J., Paelinckx, D., Mücher, C.A., Kooistra, L., Haest, B., De Blust, G., Schmidt, A.M., 2011. Integrating remote sensing in Natura 2000 habitat monitoring: Prospects on the way forward. J. Nat. Conserv. 19, 116–125. https://doi.org/10.1016/j.jnc.2010.07.003

Vrieling, A., Meroni, M., Darvishzadeh, R., Skidmore, A.K., Wang, T., Zurita-Milla, R., Oosterbeek, K., O'Connor, B., Paganini, M., 2018. Vegetation phenology from Sentinel-2 and field cameras for a Dutch barrier island. Remote Sens. Environ. 215, 517–529. https://doi.org/10.1016/j.rse.2018.03.014

Wakulińska, M., Marcinkowska-Ochtyra, A., 2020. Multi-temporal sentinel-2 data in classification of mountain vegetation. Remote Sens. 12. https://doi.org/10.3390/RS12172696

Wittke, S., Yu, X., Karjalainen, M., Hyyppä, J., Puttonen, E., 2019. Comparison of two-dimensional multitemporal Sentinel-2 data with three-dimensional remote sensing data sources for forest inventory parameter estimation over a boreal forest. Int. J. Appl. Earth Obs. Geoinf. 76, 167–178. https://doi.org/10.1016/j.jag.2018.11.009

Yeo, S., Lafon, V., Alard, D., Curti, C., Dehouck, A., Benot, M.-L., 2020. Classification and mapping of saltmarsh vegetation combining multispectral images with field data. Estuar. Coast. Shelf Sci. 236, 106643. https://doi.org/https://doi.org/10.1016/j.ecss.2020.106643

Zlinszky, A., Schroiff, A., Kania, A., Deák, B., Mücke, W., Vári, Á., Székely, B., Pfeifer, N., 2014. Categorizing grassland vegetation with full-waveform airborne laser scanning: A feasibility study for detecting natura 2000 habitat types. Remote Sens. 6, 8056–8087. https://doi.org/10.3390/rs6098056

Appendices

Appendix A. Typology of habitats in the Loire Estuary. The EUR28 habitats, marked in bold, represent the priority habitats of community interest. Fields marked with an asterisk correspond to non-vegetated or artificialized areas. They were assigned to habitat typologies based on the biotope using the criteria of the French EUNIS habitat determination guide (Gayet et al., 2018) and the 'Cahiers d'habitats' (Bensettiti et al., 2001–2005).

Physiognomic units	Phytosociological units	EUNIS habitats	EUR 28 habitats
Marine habitats	*Sandy shore comprising clean sands (coarse, medium or fine-grained) and muddy sands	A2.2 - Littoral sand and muddy sand	1130 - Estuaries
	*Muddy shores of fine particulate sediment, mostly in the silt and clay fraction	A2.3 - Littoral mud	
	Thero – Salicornietalia dolichostachyae Tüxen *ex* Boullet & Géhu 2004	A2.551 - *Salicornia* , *Suaeda* and *Salsola* pioneer saltmarshes	1310 - *Salicornia* and other annuals colonising mud and sand
	Parapholido strigosae – Hordeetum marini (Géhu et al. 1975) Géhu & de Foucault 1978	A2.553 - Atlantic *Sagina maritima* communities	
	Puccinellietum maritimae Christiansen 1927	A2.542 - Atlantic lower shore communities	1330 - Atlantic salt meadows (*Glauco-Puccinellietalia maritimae*)
	Halimionion portulacoidis Géhu 1976	A2.527 - Atlantic salt scrubs	
	Armerion maritimae Braun-Blanquet & De Leeuw 1936	A2.531 - Atlantic upper shore communities	
	Glauco maritimi – Juncion maritimi Géhu & Géhu-Franck ex Géhu in Bardat et al. 2004		
	Agropyrion pungentis Géhu 1968	A2.511 - Atlantic saltmarsh and drift rough grass communities	
	Atriplicion littoralis Nordhagen 1940	A2.512 - Atlantic saltmarsh driftline annual communities	
	Alopecurion utriculati Zeidler 1954	A2.523 - Mediterranean short *Juncus* , *Carex* , *Hordeum* and *Trifolium* saltmeadows	1410 - Mediterranean salt meadows (*Juncetalia maritimi*)
	Ranunculo ophioglossifolii – Oenanthion fistulosae de Foucault in de Foucault & Catteau 2012		
	Atriplici laciniatae – Salsolion kali Géhu 1975	B1.12 - Middle European sand beach annual communities	2110 - Embryonic shifting dunes
	Honckenyo peploidis – Elymion arenarii Tüxen 1966	B1.31 - Embryonic shifting dunes	
	Ammophilion arenariae (Tüxen in Braun-Blanquet & Tüxen 1952) Géhu 1988	B1.32 - White dunes	2120 - Shifting dunes along the shoreline with *Ammophila arenaria* (white dunes)
	Euphorbio portlandicae-Helichrysion stoechadis Géhu et Tx. *ex* Sissingh 1974	B1.42 - Biscay fixed grey dunes	**2130 - Fixed coastal dunes with herbaceous vegetation (grey dunes)**
Waterbodies and reedbeds habitats	*Open fresh or brackish waterbodies	C - Inland surface waters	
	*Loire river subject to the tid	X01 - Estuaries	
	Lemnetalia minoris Tüxen *ex* O. Bolòs & Masclans 1955	C1.22 - Free-floating vegetation of mesotrophic waterbodies	3150 - Natural eutrophic lakes with *Magnopotamion* or *Hydrocharition* -type vegetation
	Hydrocharition morsus-ranae Rübel *ex* Klika in Klika & Hadač 1944	C1.23 - Rooted submerged vegetation of mesotrophic waterbodies	
	Potamion pectinati (W. Koch 1926) Libbert 1931	C1.33 - Rooted submerged vegetation of eutrophic waterbodies	
	Ranunculion aquatilis H. Passarge *ex* Theurillat in Theurillat, Mucina & Hájek 2015		
	Nymphaeion albae Oberd. 1957	C1.24 - Rooted floating vegetation of mesotrophic waterbodies	
	Phragmitetum communis Savič 1926 and *Astero tripolii – Phragmitetum communis* Jeschke *ex* Krisch 1974	C3.21 - *Phragmites australis* beds	
	Scirpetum lacustris Chouard 1924	C3.22 - Scirpus lacustris beds	
	Typhetum latifoliae Nowiński 1930 and *Typhetum angustifoliae* P.Allorge *ex* Pignatti 1953	C3.23 - Typha beds	
	Eleocharito palustris – Sagittarion sagittifoliae Passarge 1964 and *Iridetum pseudacori* Eggler *ex* Brzeg & M.Wojterska 2001 and *Equisetetum eleocharitis* Nowiński 1930	C3.24 - Medium-tall non-graminoid waterside communities	
	Glycerietum aquaticae Nowiński 1930	C3.251 - Sweetgrass beds	
	Glycerietum fluitantis Nowiński 1930	C3.1 - Species-rich helophyte beds	
	Phalaridion arundinaceae Kopecký 1961	C3.26 - *Phalaris arundinacea* beds	
	Scirpion maritimi Dahl & Hadač 1941	C3.27 - Halophile *Scirpus* , *Bolboschoenus* and *Schoenoplectus* beds	
	Heleochloion schoenoidis Braun-Blanquet *ex* Rivas Goday, Borja, Monasterio, Galiano & Rivas-Martínez 1956	C3.423 - Mediterranean amphibious crypsis swards	**3170 - Mediterranean temporary ponds**
	Bidention tripartitae (W. Koch 1926) Nordhagen 1940 and *Chenopodion rubri* (Tüxen in Poli & J. Tüxen 1960) Hilbig & Jage 1972	C3.5 - Periodically inundated shores with pioneer and ephemeral vegetation	
	Elatino triandrae – Damasonion alismatis de Foucault 1988	C3.51 - Euro-Siberian dwarf annual amphibious swards	3130 - Oligotrophic to mesotrophic standing waters with vegetation of the *Littorelletea uniflorae* and/or *Isoeto-Nanojuncetea*
	Radiolion linoidis W. Pietsch 1971		
	*Mud bottoms of waterbodies	C3.6 - Unvegetated or sparsely vegetated shores with soft or mobile sediments	
	Caricion gracilis Neuhäusl 1959 and *Carici pseudocyperi - Rumicion hydrolapathi* H. Passarge 1964	D5.21 - Beds of large *Carex spp.*	
Grasslands habitats	*Thero – Airion* Tüxen ex Oberdorfer 1957	E1.91 - Dwarf annual siliceous grassland	
	Mesophile hay meadows (Cynosurion cristati Tüxen 1947; Lolio perennis – Plantaginion majoris G. Sissingh 1969)	E2.1 - Permanent mesotrophic pastures and aftermath-grazed meadows	
	Cynosurion cristati Tüxen 1947 X Grp des *Sisymbrietea officinalis*	E2.1 - Permanent mesotrophic pastures and aftermath-grazed meadows X E5.1 - Anthropogenic herb stands	
	*Land occupied by heavily fertilised or reseeded permanent grasslands	E2.6 - Agriculturally-improved, re-seeded and heavily fertilised grassland, including sports fields and grass lawns	
	Oenanthion fistulosae de Foucault 2008	E3.41 - Atlantic and sub-Atlantic humid meadows and	
	Bromion racemosi Tüxen ex de Foucault 2008		
	Ranunculo repentis – Cynosurion cristati Passarge 1969		
	Wet and humid meadows dominated by *Juncus effusus*	E3.417 - Soft rush meadows	
	Hygrophilic pastures regularly flooded by the oligohaline water of Loire River and dominated by *Agrostis stolonifera*	E3.44 - Flood swards and related communities	
	Meso-hygrophilic pastures regularly flooded by the oligohaline water of Loire River and dominated by *Agrostis stolonifera*		
	Mentho longifoliae – Juncion inflexi Th. Müll. & Görs ex de Foucault 2008		
	Potentillion anserinae Tüxen 1947		
	Pastures regularly flooded by the oligohaline water of Loire River and dominated by Juncus inflexus	E3.441 - Tall rush pastures	
	Hygrophilic pastures regularly flooded by the brackish water of Loire River and dominated by *Agrostis stolonifera*	E3.44 - Flood swards and related communities X A2.5 - Coastal saltmarshes and saline reedbeds	
	Meso-hygrophilic pastures regularly flooded by the brackish water of Loire River and dominated by *Agrostis stolonifera*		
	Juncion acutiflori Braun-Blanquet in Braun-Blanquet & Tüxen 1952	E3.512 - Acidocline purple moorgrass meadows	6410 - *Molinia* meadows on calcareous, peaty or clayey-siltladen soils (*Molinion caeruleae*)
	Sisymbrietea officinalis Korneck 1974 and *Convolvulo arvensis – Agropyrion repentis* Görs 1966	E5.1 - Anthropogenic herb stands	

	Achilleo ptarmicae – Cirsion palustris Julve & Gillet ex de Foucault 2011	E5.412 - Western nemoral river bank tall-herb communities dominated by *Filipendula*	6430 - Hydrophilous tall herb fringe communities of plains and of the montane to alpine levels
	Convolvulion sepium Tüxen in Oberdorfer 1957		
	Thalictro flavi – Filipendulion ulmariae de Foucault in Royer et al. 2006		
	Calystegio sepium – Althaeion officinalis de Foucault 2011	E5.4112 - *Angelica heterocarpa* fluvial communities	
	Aegopodion podagrariae Tüxen 1967	E5.43 - Shady woodland edge fringes	
	Holco mollis – Pteridion aquilini Passarge (1994) 2002	E5.3 - *Pteridium aquilinum* fields	
Scrubs and thickets habitats	*Solano dulcamarae – Tamaricetum gallicae* de Foucault 2008	F9.3131 - West Mediterranean tamarisk thickets	92D0 - Southern riparian galleries and thickets (*Nerio - Tamaricetea* and *Securinegion tinctoriae*)
	Species-poor *Prunus spinosa* or *Rubus spp.* thickets	F3.111 - Blackthorn-bramble scrub	
	Ulici europaei - Cytisetum scoparii Oberdorfer ex B. Foucault, Lazare & Bioret 2013	F3.14 - Temperate *Cytisus scoparius* fields	
	Ulici europaei – Prunetum spinosae Géhu & Géhu-Franck 1983	F3.15 - *Ulex europaeus* thickets	
	Salicetum triandro – viminalis (Tüxen 1931) Lohmeyer 1952 ex Moor 1958	F9.121 - lmond willow-osier scrub	
	Low woods and scrubs dominated by *Salix atrocinerea*	F9.2 - *Salix* carr and fen scrub	
Woodland and forest habitats	*Salicion albae* Soó 1930	G1.1111 - Western European white willow forests	**91E0 - Alluvial forests with *Alnus glutinosa* and *Fraxinus excelsior* (*Alno-Padion*, *Alnion incanae*, *Salicion albae*)**
	Alnenion glutinoso - incanae Oberdorfer 1953	G1.211 - *Fraxinus - Alnus* woods of rivulets and springs	
	Ulmo laevis – Fraxinetum angustifoliae (Breton) Rameau & Schmitt ex J.-M. Royer, Felzines, Misset & Thévenin 2006	G1.22 - Mixed *Quercus - Ulmus - Fraxinus* woodland of great rivers	91F0 - Riparian mixed forests of *Quercus robur*, *Ulmus laevis* and *Ulmus minor*, *Fraxinus excelsior* or *Fraxinus angustifolia*, along the great rivers (*Ulmenion minoris*)
	Meso-hygrophilic forests dominated by *Quercus robur* and *Fraxino excelsioris – Quercion roboris* Rameau 1996	G1.A1 - *Quercus - Fraxinus - Carpinus* betulus woodland on eutrophic and mesotrophic soils	
	Ulmus minor thickets	G1.A61 - *Ulmus minor* woods	
	Plantations of species, hybrids or cultivars of the deciduous genus *Populus*	G1.C1 - *Populus* plantations	
	Plantations of Palaearctic conifers of genus *Pinus*	G3.F12 - Native pine plantations	
Cultived agricultural habitats	Cereal crops	I1.1 - Intensive unmixed crops	

Appendix B. MDG measures obtained after RF classification for the nine analyzed dates. The five most contributing variables, which have been retained to integrate the temporal series, are marked in bold.